

Distribution Categories:  
Magnetic Fusion Energy (UC-20)  
MFE—Fusion Systems (UC-20d)

ANL/FPP/TM-169

ANL/FPP/TM--169

DE83 016711

ARGONNE NATIONAL LABORATORY  
9700 South Cass Avenue  
Argonne, Illinois 60439

**TOKAMAK FUSION REACTORS WITH LESS THAN FULL TRITIUM BREEDING**

by

K. Evans, Jr., J. G. Gilligan,\*  
and J. Jung

Fusion Power Program

May 1983

**MASTER**

\*Faculty Research Participant, Summer 1982. Present address: NC State  
University, Raleigh, N. C.

DISTRIBUTION OF THIS DOCUMENT IS UNLIMITED

*Reg*

## **DISCLAIMER**

This report was prepared as an account of work sponsored by an agency of the United States Government. Neither the United States Government nor any agency thereof, nor any of their employees, makes any warranty, express or implied, or assumes any legal liability or responsibility for the accuracy, completeness, or usefulness of any information, apparatus, product, or process disclosed, or represents that its use would not infringe privately owned rights. Reference herein to any specific commercial product, process, or service by trade name, trademark, manufacturer, or otherwise does not necessarily constitute or imply its endorsement, recommendation, or favoring by the United States Government or any agency thereof. The views and opinions of authors expressed herein do not necessarily state or reflect those of the United States Government or any agency thereof.

## TABLE OF CONTENTS

	<u>Page</u>
ABSTRACT . . . . .	1
I. INTRODUCTION . . . . .	2
II. REACTOR DESIGN CRITERIA AND DESIGN TRADEOFFS . . . . .	4
III. METHOD OF ANALYSIS . . . . .	7
IV. REACTOR DESIGNS . . . . .	7
A. Definition of TBR . . . . .	7
B. Determination of Operating Temperature . . . . .	9
C. Determination of Blanket/Shield Characteristics . . . . .	12
D. Specific Reactor Designs . . . . .	20
V. TRITIUM CONSIDERATIONS . . . . .	27
VI. COSTING . . . . .	29
VII. SUMMARY AND CONCLUSIONS . . . . .	34
ACKNOWLEDGMENTS . . . . .	37
REFERENCES . . . . .	38

## LIST OF TABLES

<u>No.</u>	<u>Title</u>	<u>Page</u>
I	Comparison of Steady-State D-T and Cat-D Reactor Designs .....	2
II	Design Tradeoffs .....	6
III	First-Wall/Blanket/Shield Model .....	14
IV	Tritium Concentrations Used for the Specific Designs and Related Quantities .....	22
V	Costing Model Results for STARFIRE and WILDCAT .....	32

## LIST OF FIGURES

<u>No.</u>	<u>Title</u>	<u>Page</u>
1	Approximate expression for the tritium breeding ratio as a function of tritium concentration. ....	9
2	Reactor temperatures as a function of $r_T$ . ....	11
3	Geometric configuration of the inboard blanket/shield. ....	13
4	Absorbed nuclear dose in the epoxy insulation for the toroidal field magnets. ....	15
5	Tritium breeding ratio obtained with a given outboard breeding blanket thickness - liquid lithium breeder. ....	16
6	Tritium breeding ratio obtained with a given outboard breeding blanket thickness - Li <sub>2</sub> O breeder. ....	17
7	Outboard energy deposition - liquid lithium breeder. ....	18
8	Outboard energy deposition - Li <sub>2</sub> O breeder. ....	19
9	Inboard blanket/shield thickness and energy multiplication. ....	21
10	Major radius as a function of tritium concentration for fixed thermal power and first-wall heat load. ....	25
11	Peak toroidal field as a function of tritium concentration for fixed thermal power and fixed wall heat load. ....	26
12	Rates of tritium burnup, production, exhaust, and fueling. ....	28
13	Tritium inventories. ....	30
14	Cost analysis. ....	32

## **TOKAMAK FUSION REACTORS WITH LESS THAN FULL TRITIUM BREEDING**

K. Evans, Jr., J. G. Gilligan, and J. Jung

### **ABSTRACT**

A study of commercial, tokamak fusion reactors with tritium concentrations and tritium breeding ratios ranging from full deuterium-tritium operation to operation with no tritium breeding is presented. The design basis for these reactors is similar to those of STARFIRE and WILDCAT. Optimum operating temperatures, sizes, toroidal field strengths, and blanket/shield configurations are determined for a sequence of reactor designs spanning the range of tritium breeding, each having the same values of beta, thermal power, and first-wall heat load. Additional reactor parameters, tritium inventories and throughputs, and detailed costs are calculated for each reactor design. The disadvantages, advantages, implications, and ramifications of tritium-depleted operation are presented and discussed.

## I. INTRODUCTION

The two commercial, tokamak, reactor studies, STARFIRE<sup>1</sup> and WILDCAT,<sup>2</sup> represent the extremes of a continuum of possible reactor designs parameterized by the relative tritium content,  $r_T = \bar{n}_D/\bar{n}_T$ , of the plasma. STARFIRE has  $r_T = 1.0$ , the choice which optimizes the plasma performance given that sufficient tritium can be bred and extracted from the blanket to maintain this value. WILDCAT has  $r_T = 4.8 \times 10^{-3}$ , the value that naturally occurs for a Cat-D device where no tritium is bred. In WILDCAT all of the tritium produced by the reaction,  $D + D \rightarrow p + T$ , is eventually burned in the plasma, either before it diffuses out or after it is reinjected. A summary of important parameters for STARFIRE and WILDCAT is shown in Table I.

TABLE I  
Comparison of Steady-State D-T and Cat-D Reactor Designs

	STARFIRE	WILDCAT
Fuel cycle	D-T	Cat-D
$r_T = \bar{n}_D/\bar{n}_T$	1.0	$4.8 \times 10^{-3}$
Major radius, m	7.0	8.58
Aspect ratio	3.6	3.25
Peak toroidal field, T	11.1	14.35
Plasma toroidal average beta	0.067	0.11
Average electron temperature, keV	17.3	30.0
Plasma current, MA	10.1	29.9
Thermal power, GW(thermal)	4.0	2.9
Net electric power, MW(electrical)	1200	810
Tritium inventory, g	11,400	45
Normal tritium release, Ci/d	13	0.31
Cost of electricity, (1980) mills/kWh	35.1	62.8

STARFIRE and D-T reactors in general have the advantages of higher power density, lower  $n\tau$  for ignition, and lower plasma temperatures, leading to a more attractive reactor with a lower cost of electricity. WILDCAT and Cat-D reactors eliminate the problems associated with breeding tritium and have

greatly reduced tritium inventories and tritium releases. In addition, the inboard blanket/shield can be made thinner and somewhat higher neutron energy multiplication can be obtained. It is interesting to look at reactors with intermediate values of  $r_T$  for several reasons: First, it may not be possible to breed, extract, and reinject sufficient tritium to maintain  $r_T = 1$ . Such a tritium system, even though it is indicated in most D-T reactor designs, is a far from demonstrated fact. For example, liquid lithium and lithium alloy blankets must deal with safety, corrosion, and pumping problems, and tritium breeding and extraction may be difficult for solid breeders. One, hence, may be forced to values of  $r_T < 1$ , especially in near-term designs. Second, it is useful to determine the extent of the penalty one pays for breeding lesser amounts of tritium. Third, examination of the intermediate cases results in a better understanding of both the D-T and D-D cases and the factors which distinguish them.

The purpose of this study is to examine a number of intermediate cases between and including a D-T reactor (as much as possible like STARFIRE) and a Cat-D reactor (as much as possible like WILDCAT.) Relatively detailed design parameters have been developed so that reasonably accurate costs can be determined. The reactor subsystems have been modeled in such a way that their important parameters can be scaled to a large extent from STARFIRE and WILDCAT using a consistent set of design philosophies and assumptions.

Previous work has been done by Greenspan<sup>3</sup> on the concept of adding tritium to a Cat-D plasma (tritium-assisted operation) in order to reduce the ignition requirements and increase the fusion power density. However, the results were generic in nature and details of the full reactor designs were not undertaken. Conn<sup>4</sup> and Cohn<sup>5</sup> have also noted that there may be a continuum of reactors with  $r_T < 1$  between D-T and Cat-D.

The choice of a standard set of parameters for the reactor designs is discussed in Sec. II, and the calculational methods are described in Sec. III. Section IV discusses the relationship between the tritium concentration,  $r_T$ , and the breeding ratio, the determination of the optimum operating temperature and the blanket/shield characteristics for specific values of  $r_T$ , and a description of the nine reference design points covering the range from full to no tritium breeding. Tritium inventories and throughputs are covered in Sec. V, and a cost analysis is presented in Sec. VI, with a summary and major conclusions of the study being listed in Sec. VII.

## II. REACTOR DESIGN CRITERIA AND DESIGN TRADEOFFS

The STARFIRE and WILDCAT tokamak reactor designs are used as the basis for our study. However, these two designs are not totally consistent with each other (with respect to choice of beta, choice of operating temperature, etc., see Table I), and so some standardization has been made. Without standardization the effects of changes in  $r_T$  (or tritium breeding ratio) can be masked by inconsistent assumptions.

The first assumption that is made is to choose the average toroidal beta,  $\beta_t$ , to be 10% for all the reactors including the D-T and Cat-D base design reactors. The reason for taking a single value for beta is that it is not felt that beta is a design choice. Any reactor would operate at the highest practical value of beta, which is not known at this time, and that value should be about the same for all reactors with similar plasma cross sections and aspect ratios. For STARFIRE  $\beta_t$  was 6.7% and for WILDCAT it was 11%. Hence, the fusion power density of our D-T reactor is higher than that of STARFIRE, and that of the Cat-D reactor is somewhat lower than that of WILDCAT. Other MHD parameters, such as aspect ratio, safety factor, and D-shapedness, differ slightly between STARFIRE and WILDCAT. We have chosen a consistent set of MHD parameters for use in this study. These include aspect ratio,  $A = 3.25$ ; elongation,  $\kappa = 1.6$ ; D-shapedness,  $d = 0.2$ ; safety factor,  $q(a) = 3.0$  and  $q(0) = 1.0$ ; and pressure profile exponent,  $\alpha_p = 1.4$ .<sup>6</sup> These values are for the most part those of WILDCAT and are felt to be more general than those of STARFIRE, which were chosen to optimize the lower-hybrid current drive in that device. The less D-shaped plasma cross section makes the equilibrium field coil design easier, and probably does not detract greatly from the possibility of achieving a high beta.

The heat load on the first wall has been found to be a limiting design constraint for both STARFIRE and WILDCAT. Hence, we choose the same design criteria, that all radiation and charged particles emitted from the plasma not contribute more than  $1 \text{ MW/m}^2$  to the first wall loading. As a consequence, the total first wall loadings (including neutrons) for our D-T and Cat-D designs are insignificantly different from those of STARFIRE and WILDCAT, respectively.

Total thermal power (plasma plus blanket) has been fixed at 4000 MWt for our designs. This is the same as for STARFIRE but greater than for WILDCAT

(2915 MWt). This size plant was chosen for STARFIRE as being that typically desired by utility companies.<sup>1</sup> This assumption is desirable (though not essential) to facilitate comparison between designs. It has the effect of increasing the size of the Cat-D plant relative to WILDCAT. Other general guidelines followed for STARFIRE and WILDCAT have also been observed here. These include the assumption of steady-state operation.

The current drive method has been assumed to be relativistic electron beams (REB) as postulated for DEMO.<sup>7</sup> An REB system is predicted to be highly efficient and does not heat the plasma significantly in order to drive the current. There is some preliminary experimental evidence supporting REB current drive, but like all current drive schemes, it should be considered as requiring further research to establish its credibility. STARFIRE used a lower-hybrid-wave, current drive, which is too inefficient for a D-D reactor, and WILDCAT used Alfvén waves, which are more efficient but also more speculative, for current drive. The REB system, if its potential is realized, would be more attractive for both these reactors. The alternative to a steady-state, current driven reactor is a pulsed, ohmically-driven device, which has many disadvantages, including significantly higher cost due to the large power supplies and required thermal storage as documented in the WILDCAT study.<sup>2</sup>

The impurity level of beryllium (from the pumped limiter) in the plasma has been set at 3% as was used in the previous designs. For the most part all other systems have been assumed to be similar to STARFIRE and WILDCAT, involving parameters intermediate to the two designs.

Shown in Table II is a listing of some of the major design tradeoffs one is expected to observe as  $r_T$  is decreased from unity (D-T reactor) toward a low value corresponding to operation in a Cat-D mode. These, in general, are the same design advantages and disadvantages observed for WILDCAT when compared to STARFIRE. One of the major contributions of this study is to determine quantitatively where the tradeoffs occur. One of the important positive effects of a reduced tritium concentration is the ability to have a less thick inner blanket/shield. This was shown to be very beneficial in the design of WILDCAT (a 1-cm decrease in thickness resulted in an increase of ~1% in thermal power). In addition, with a lower required tritium breeding ratio one can increase the neutron energy multiplication by using materials which enhance this property (e.g. steel rather than lithium.) Thus while ~40% of the total

fusion power from a Cat-D plasma is from neutrons, the blanket energy multiplication in WILDCAT led to a neutron contribution of ~52% to the thermal power. Perhaps the most important advantage of operating with a reduced tritium breeding ratio is the resulting reduced tritium inventory. However, even for a D-D reactor, the tritium permeates the reactor system and must be controlled. The level for which tritium becomes of negligible concern is still a somewhat open question. In this report the tritium inventory is calculated as a function of  $r_T$ , and significantly low values are noted.

The negative effects of plasma operation with depleted tritium are also shown in Table II. The most important of these is the reduction in fusion power density. The resulting power loss can be made up in essentially two main ways: (1) by increasing the toroidal field via stronger magnets or thinner inboard blanket/shield (the power is proportional to the fourth power of the field); and (2) by increasing the plasma size (the power is proportional to the plasma volume). The beneficial effects of a thinner blanket/shield and higher neutron energy multiplication, while helpful, do not significantly restore the lowered power density. The required increases in magnetic field and size, then, eventually lead to a higher cost of electricity.

TABLE II

Design Tradeoffs

(Observed when  $r_T = \bar{n}_T/\bar{n}_D$  is decreased from D-T toward Cat-D operation. Total thermal power, wall load, and  $\beta_c$  are fixed.)

Positive Effects	Negative Effects
● Tritium breeding ratio (decreased)	● Fusion power density (decreased)
● Inner blanket and shield thickness (decreased)	● Toroidal magnetic field (increased)
● Neutron energy multiplication (increased)	● Plasma size (increased)
● Tritium inventory (decreased)	● Plasma operating temperature (increased)
● Tritium release (decreased)	● Ignition margin (decreased)
	● Required $n\tau$ (increased)

### III. METHOD OF ANALYSIS

The same general procedure used to design both STARFIRE and WILDCAT is followed here. A profile-averaged, steady-state, reactor analysis code, TRAC-II, is used to determine the basic plasma parameters. Averages over specified plasma profiles are used to obtain the global, multispecies, particle and energy balance equations solved by TRAC-II. The averaging is done over the actual flux surfaces of the MHD equilibrium, and the power and particle balance and the MHD equilibrium are handled consistently. A charged particle slowing-down model calculates energy deposited in thermal ions or electrons by superthermal fusion products. Superthermal fusions are also accounted for. A detailed toroidal field coil model is used to size the toroidal field superconducting magnets.<sup>8</sup> The TRAC-II code was also used for the STARFIRE and WILDCAT designs.

The neutronics analysis for calculation of the tritium breeding ratio and shielding requirements has employed the one-dimensional code ANISN<sup>9</sup> with the  $S_8P_3$  approximation. The cross-section libraries for the particle transport<sup>10</sup> and the nuclear response function<sup>11</sup> used for the analysis consist of 46 neutron groups and 21 gamma groups.

In addition, a detailed cost algorithm has been used in this study. The costing is done on the same basis and with the same assumptions as for STARFIRE and WILDCAT. The costs obtained should be directly comparable to those obtained for STARFIRE and WILDCAT.

### IV. REACTOR DESIGNS

#### A. Definition of TBR

We begin by first relating the plasma tritium concentration,  $r_T = \bar{n}_T/\bar{n}_D$ , to the required tritium breeding ratio (TBR), which is defined as the net number of tritons burned in the plasma divided by the total number of neutrons (including both 14.06-MeV and 2.45-MeV neutrons) produced in the plasma. It should be noted that this definition of tritium breeding ratio is that required by the plasma and does not take into account any of the details of breeding or extracting tritium from a blanket, nor of reinjecting tritium into the plasma. It is not the same breeding ratio as commonly defined in neutronics studies. For a

steady-state system in which all the tritium that diffuses out of the plasma is recycled or reinjected, an approximate expression for the TBR as a function of  $r_T$  and the ion temperature is

$$\text{TBR} \approx \frac{r_T \langle \sigma v \rangle_{DT} - (1/2) \langle \sigma v \rangle_{DD}^T}{r_T \langle \sigma v \rangle_{DT} + (1/2) \langle \sigma v \rangle_{DD}^n}, \quad (1)$$

where  $\langle \sigma v \rangle_{DT}$ ,  $\langle \sigma v \rangle_{DD}^T$ , and  $\langle \sigma v \rangle_{DD}^n$  are the reactivities for the D-T, D-D (T branch) and D-D (n branch) fusion reactions, respectively. Equation (1) assumes a uniform plasma (i.e. ignores profile effects) and neglects superthermal fusions. Shown in Fig. 1 is a plot of this expression for the TBR versus  $r_T$  for various assumed ion temperatures. The TBR is fairly constant until  $r_T$  becomes less than  $\sim 0.05$ . The value of  $r_T$  must be less than 0.1 (for  $T_i \lesssim 40$  keV) before the TBR is less than  $< 0.9$ . Alternately, it could be stated that  $r_T$  is a very sensitive function of TBR for high-values of the TBR. Unfortunately, because of this behavior a relatively small decrease in TBR near TBR = 1.0 results in a significant decrease in D-T fusion power density in the plasma.

Several other features of Fig. 1 should also be noted. For a 50-50 D-T plasma ( $r_T = 1$ ), the value of the TBR can be seen from Eq. (1) to be slightly less than unity (TBR = 0.9944, at  $T_i = 7$  keV). The reason is that a small number of tritons and a small number of neutrons are produced in the plasma from D-D reactions. If D-D reactions were ignored, the TBR would exactly be unity. For the case of Cat-D for which the TBR is zero, the value of  $r_T$  is seen to be a function of  $T_i$ . (For WILDCAT  $r_T = 4.8 \times 10^{-3}$ .) Actual values of TBR versus  $r_T$  as used in the remainder of this paper also account for the temperature and density profile effects and superthermal fusions which are not included in Eq. (1). The criteria for determining an optimum plasma operating temperature as a function of  $r_T$  is discussed in the following paragraphs. The actual values of TBR versus  $r_T$  for the designs considered fall within the envelope of lines in Fig. 1 for  $10 \text{ keV} \leq T_i \leq 50 \text{ keV}$ .

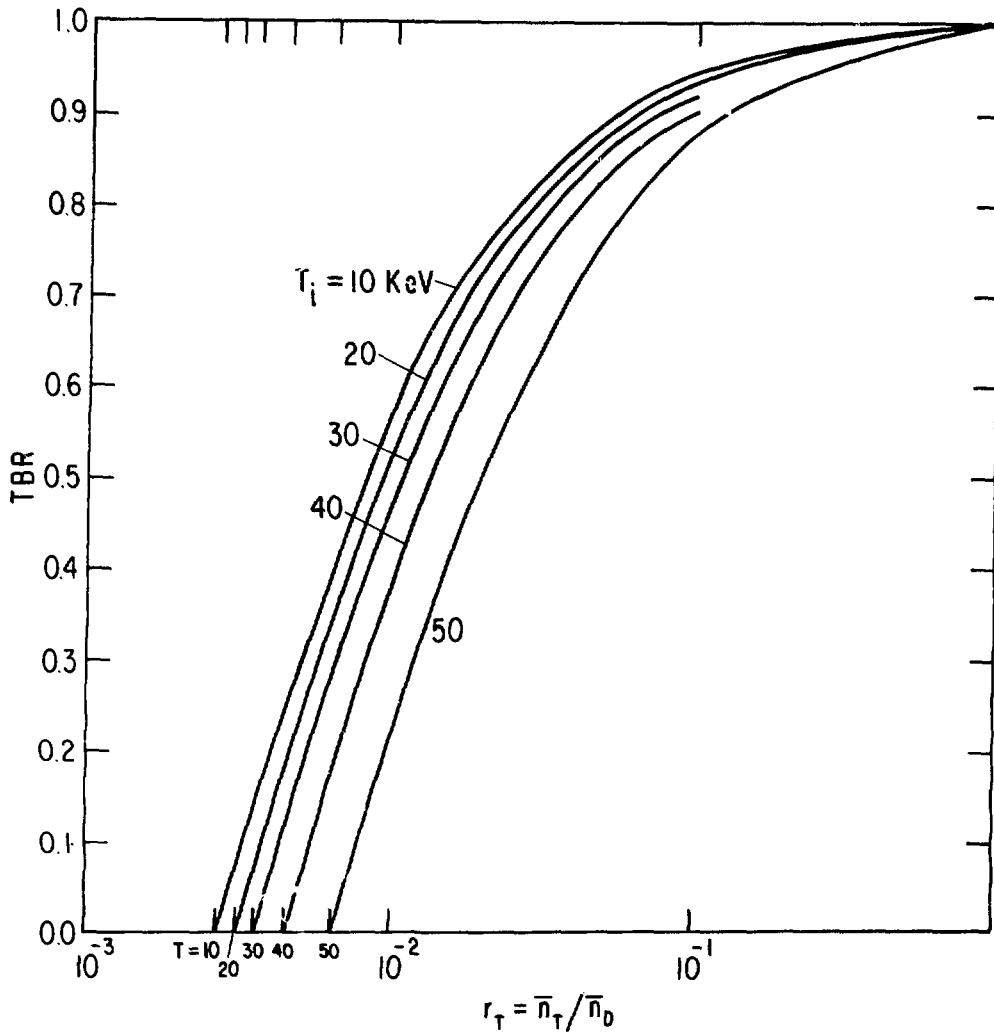


Fig. 1. Approximate expression for the tritium breeding ratio as a function of tritium concentration.

### B. Determination of Operating Temperature

The optimum temperature at which to operate a reactor is a somewhat sensitive and complicated function of  $r_T$ . A D-T reactor, for example, typically has a minimum ignition temperature near 4 keV, and the plasma fusion power density peaks near 7-8 keV. STARFIRE, on the other hand, was designed with an electron temperature of 17 keV. The reason was that at this temperature the lower-hybrid-wave current drive is significantly more effective, modifying the desire to achieve maximum power density. For the more efficient REB current drive assumed in this work, however, it should not be necessary to choose a

temperature much different from that for which the power density is a maximum. For WILDCAT, the highest power density occurs at the minimum temperature for ignition ( $\sim 25$  keV). (The ultimate power density peak, based on the maximum of the reaction rates, would occur at a lower temperature if ignition could be achieved there.) Consequently, WILDCAT is operated at a temperature of 30 keV, a few degrees above the minimum to provide a safety margin for operation.

These average temperatures depend on the density and temperature profiles. The temperature profile exponent,  $\alpha_T$ , has been taken to be 1.1 and the density profile exponent,  $\alpha_n$ , has been taken to be 0.3. This corresponds to a sharp temperature profile and a broad density profile, and the two are consistent with the fairly broad pressure profile, which has been chosen to optimize the achievement of high beta. (These choices are in lieu of determining the profiles with a transport code, a procedure that cannot be performed accurately until the relevant transport coefficients are known.) Definitions and further discussion of the effect of different profiles are treated in Refs. 2 and 12. It should be noted that the above choice of profiles is different from those for both STARFIRE and WILDCAT but is thought to be a realistic choice.

The minimum temperature for ignition and the temperature for which the peak power density occurs have been determined as a function of  $r_T$ . Typically the minimum temperature increases as  $r_T$  decreases, and below some value of  $r_T$ , the maximum power density is coincident with the minimum temperature. If all of the  $^3\text{He}$  that diffuses out is lost, then there is a minimum value of  $r_T$  below which ignition does not occur. If a reactor with a lower value of  $r_T$  is desired, some of the  $^3\text{He}$  must be reinjected. WILDCAT falls in this category, and a discussion of the reinjection of  $^3\text{He}$  is presented in Ref. 2.

The behaviors of the minimum electron temperature for ignition and the electron temperature for which the power density peaks are shown in Fig. 2. (The ion temperature is typically slightly higher than the electron temperature.) Two cases are considered, one in which no  $^3\text{He}$  is reinjected but 75% of the  $^3\text{He}$  diffusion flux is assumed to recycle naturally at the wall (see Ref. 2 for a discussion of the recycling/diffusion model) and another in which all the  $^3\text{He}$  that diffuses out is reinjected. The first case corresponds to a net recycling coefficient,  $R_3 = 0.75$ , and the second, to  $R_3 = 1.00$ . Even though reinjecting the  $^3\text{He}$  is beneficial at low values of  $r_T$ , it is deleterious for

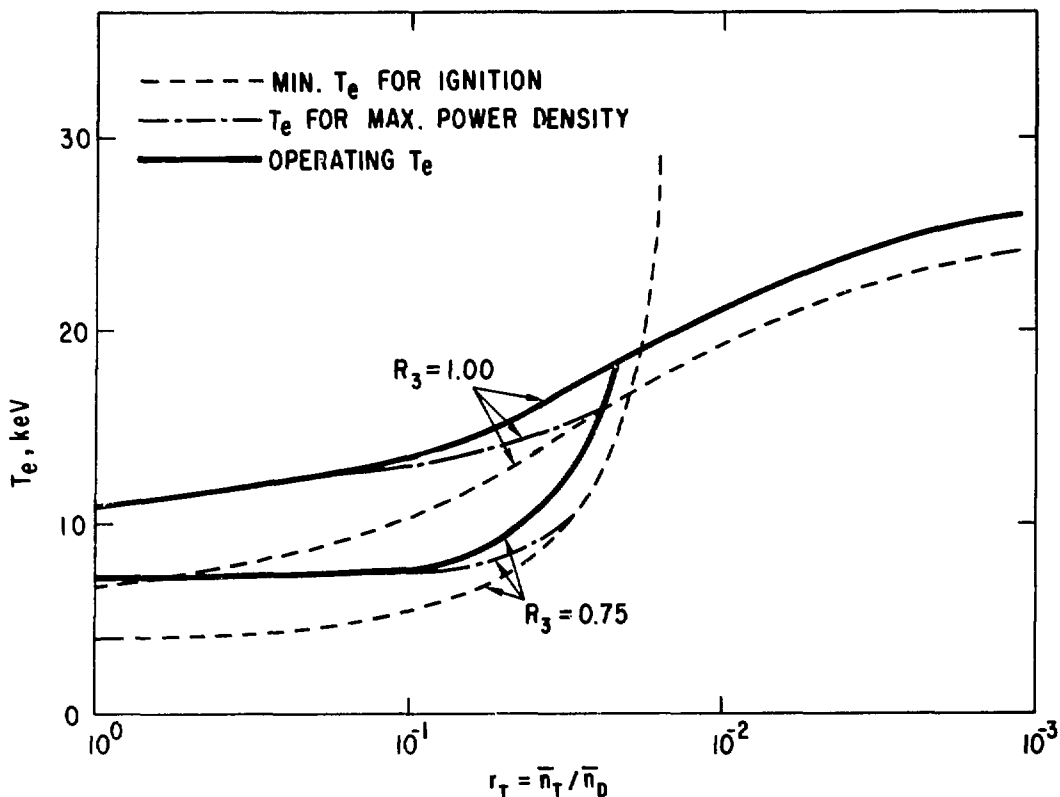


Fig. 2. Reactor temperatures as a function of  $r_T$ . The minimum temperature for ignition, the temperature for which the power density peaks, and the operating temperature for this study are shown. Catalyzation with respect to  $^3\text{He}$  ( $R_3 = 1$ ) is necessary for low values of  $r_T$ , but undesirable for values near unity.  $R_3 = 0.75$  represents the wall recycling to be expected even if no  $^3\text{He}$  is reinjected.

values of  $r_T$  close to unity. In the latter cases the power density is higher and the optimum temperature is lower for a given value of  $r_T$  than if the  $^3\text{He}$  is removed. The problem of the  $^3\text{He}$  as ash overrides its benefit as a fusion fuel. It can be noted that it is always advantageous to reinject any tritium that diffuses out, and the net tritium recycling coefficient,  $R_T$ , is consequently always taken to be unity.

It can be seen from Fig. 2 that there are three regions to be considered in the  $r_T$  dependence of the temperature. In Region I with  $1.0 \geq r_T \gtrsim 0.1$  one would want to operate with  $^3\text{He}$  removal at the temperature for which the power density peaks. This is typical of a D-T reactor. In Region III with  $0.01 < r_T$  one would like to reinject all the  $^3\text{He}$  and operate at a temperature as close as possible to the minimum temperature for ignition. This is typical of

a Cat-D reactor. The intermediate Region II with  $0.1 > r_T > 0.01$  is a transition region. The peak power density occurs near the minimum temperature for ignition and reinjection of the  $^3\text{He}$  is becoming necessary. (It can be noted that if one wants to divert  $^3\text{He}$  for "clean" D- $^3\text{He}$  satellite reactors,<sup>13</sup> then  $r_T$  must be in Region I or II.

For the purposes of this study the operating temperature as a function of  $r_T$  has been taken to be the temperature for which the power density peaks or 2-3 keV above the minimum temperature for ignition, whichever is larger. The reactors are catalyzed in  $^3\text{He}$ , that is  $R_3$  is made unity, if necessary, but not otherwise, except that both catalyzed and uncatalyzed cases are investigated near the cross-over point,  $r_T \approx 0.03$ . The chosen operating temperatures are shown in Fig. 2.

### C. Determination of Blanket/Shield Characteristics

The blanket/shield parameters which most affect the overall reactor design are the inboard blanket/shield thickness,  $\Delta_{BS}^i$ , and the two neutron energy multiplications,  $\epsilon_{14.06}$  and  $\epsilon_{2.45}$ . It is desirable to reduce the inner blanket/shield thickness in order to achieve a lower magnetic field,  $B_{TFC}$ , at the coils for the same field in the plasma. Higher neutron energy multiplication results in more power for the same device. If the power and wall loading are fixed, the result is smaller size but a higher field at the plasma which yields a net cost advantage.

The geometric layout of the inboard blanket/shield is shown in Fig. 3. The inboard shield thickness varies depending on the neutron wall loading. The quantity,  $\Delta_{BS}^i$ , is defined to be the distance between the peak field position in the inboard toroidal field magnet and the first-wall surface. It includes some of the magnet structure and also the first wall. The outboard blanket/shield is configured similarly to Fig. 3 except that the shield has a fixed thickness of 150 cm and the blanket has a fixed thickness of 70 cm divided into a breeding portion with thickness depending on the required TBR and a nonbreeding portion made of PCA stainless steel comprising the rest. The breeding portion is closest to the plasma. The composition of the various blanket/shield regions is shown in Table III. The breeding is done only in the outboard blanket, and both liquid lithium (Li) and solid (Li<sub>2</sub>O) breeders are considered. STARFIRE, which used a LiAlO<sub>2</sub> blanket, along with a neutron

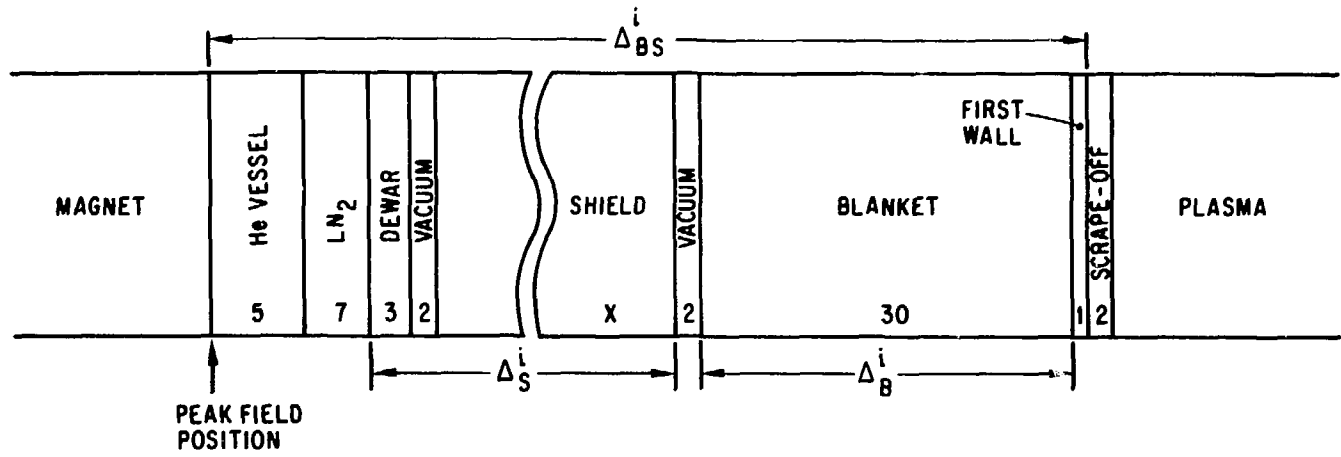


Fig. 3. Geometric configuration of the inboard blanket/shield. The shield thickness is variable.

TABLE III

First-Wall/Blanket/Shield Model

---

Inside (10% of total volume):		
First wall	1 cm	65% PCA + 35% H <sub>2</sub> O
Blanket	30 cm	90% PCA + 10% H <sub>2</sub> O
Shield	x cm	15% Fe-1422 + 15% TiH <sub>2</sub> + 10% B <sub>4</sub> C <sup>a</sup> + 55% W <sup>a</sup> + 5% H <sub>2</sub> O
Outside (90% of total volume):		
First wall	1 cm	65% PCA + 35% H <sub>2</sub> O
Blanket		
Lithium case	y cm	10% PCA + 90% Li <sup>b</sup>
	(70-y) cm	90% PCA + 10% H <sub>2</sub> O
Li <sub>2</sub> O case	y cm	10% PCA + 80% Li <sub>2</sub> O <sup>c</sup> + 10% H <sub>2</sub> O
	(70-y) cm	90% PCA + 10% H <sub>2</sub> O
Shield	150 cm	60% Fe-1422 + 35% B <sub>4</sub> C <sup>a</sup> + 5% H <sub>2</sub> O

---

<sup>a</sup>95% theoretical density (T.D.).

<sup>b</sup>100% T.D., natural lithium.

<sup>c</sup>70% T.D., natural lithium.

multiplier, required breeding in the inboard blanket, but such a ternary breeder design is not considered in this work.

It is recognized that the use of water coolant in the lithium blanket is almost certainly not feasible. This oversight was not recognized until after the study was completed. A blanket design with a more compatible coolant would change some of the results for lithium somewhat, but should not impact the trends or major conclusions of the study.

The absorbed nuclear dose in the epoxy insulation of the toroidal magnets is shown in Fig. 4 as a function of the inboard shield thickness (including the magnet dewar),  $\Delta_s^1$ . Given the reactor neutron wall loading, the required shield thickness can be determined from the information in Fig. 4. It is assumed that the plant life is 40 yr with a 75% availability and that the maximum allowable dose in the insulation is  $10^{10}$  rad. These assumptions are consistent with those for both STARFIRE and WILDCAT. This study has examined reactors with a fixed heat load on the wall. In this case the neutron wall

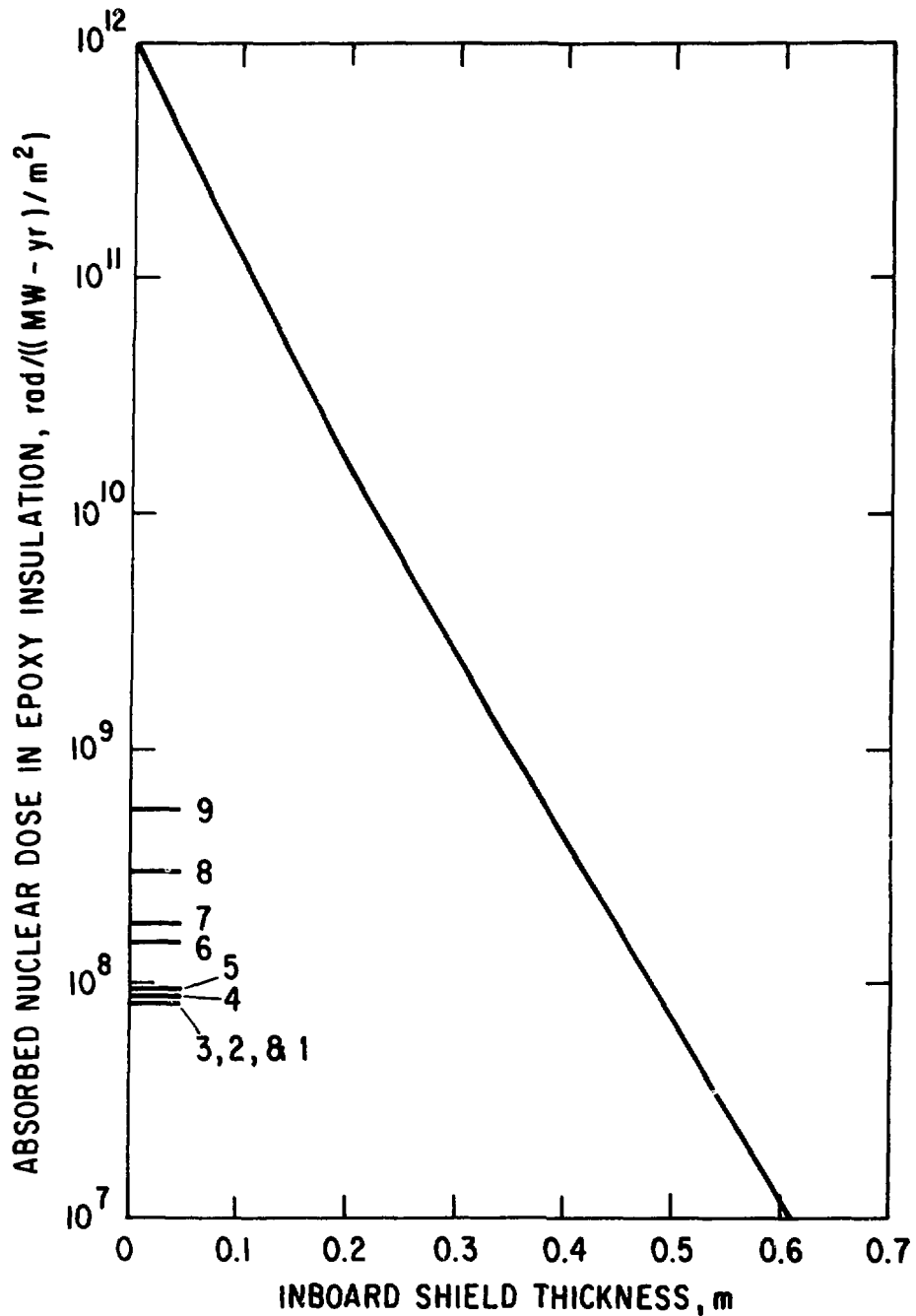


Fig. 4. Absorbed nuclear dose in the epoxy insulation for the toroidal field magnets. (The numbers 1-9 refer to values used in the specific reactor designs.)

load depends mainly on plasma characteristics associated with a given tritium concentration and given recycling of  $^3\text{He}$ . It does not depend on the size nor magnetic field of the reactor. Consequently, the shield thickness is a unique function of  $r_T$  and  $R_3$ . (Other parameters, such as impurity concentration, which could affect the plasma characteristics are not varied here.)

Figures 5 and 6 show the TBR as a function of the thickness of the breeding portion of the outboard blanket for both breeder materials. The different cases correspond to specific values of  $r_T$  and  $R_3$  to be discussed in Sec. IV.D. The TBR is also uniquely determined by  $r_T$  and  $R_3$ , so the required thickness of the breeding blanket as a function of  $r_T$  and  $R_3$  can be determined from the information in Figs. 5 and 6. These calculations indicate that both lithium and  $\text{Li}_2\text{O}$  systems can yield sufficient TBR's solely in the outboard sections

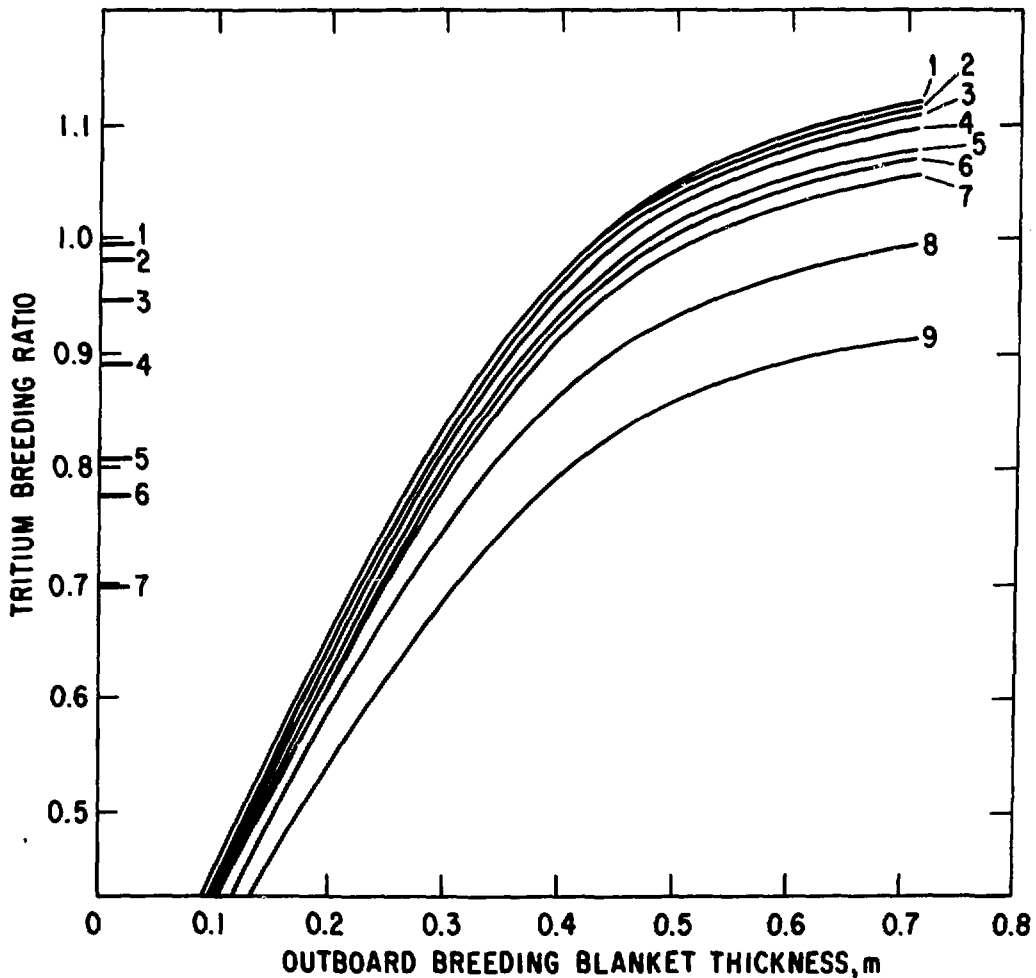


Fig. 5. Tritium breeding ratio obtained with a given outboard breeding blanket thickness - liquid lithium breeder.

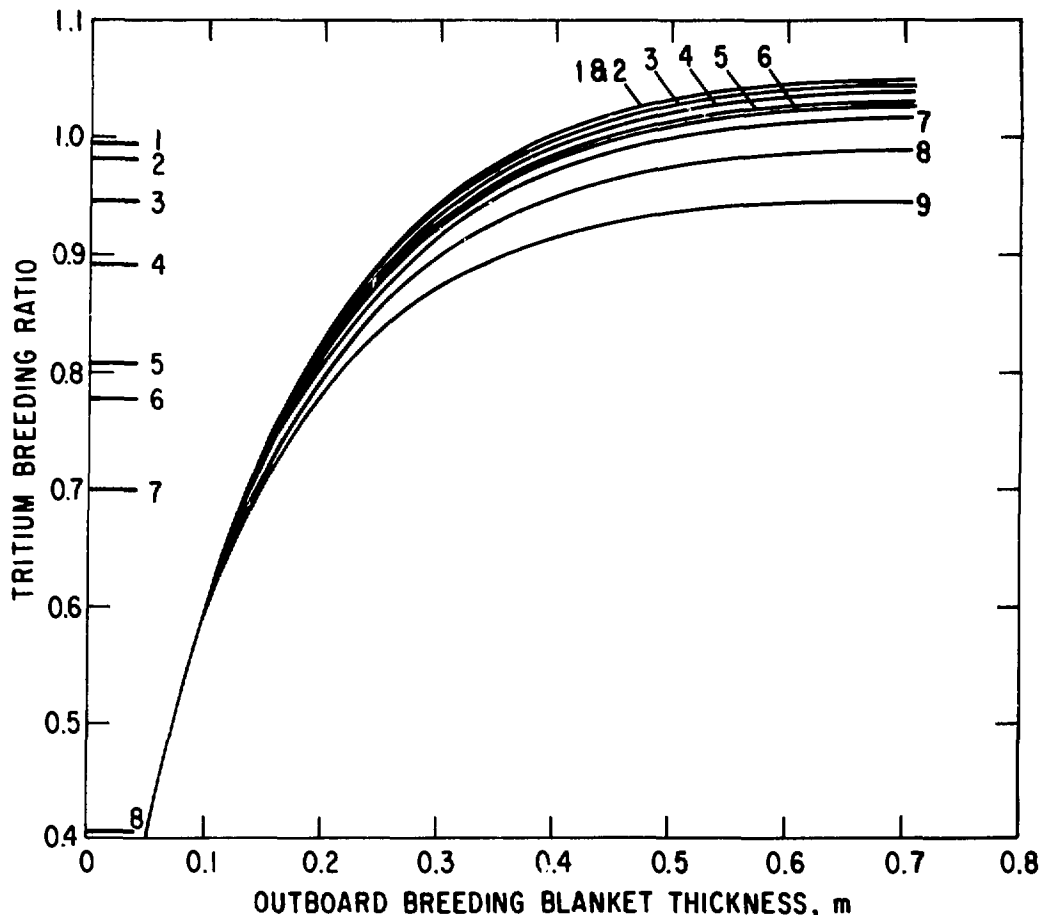


Fig. 6. Tritium breeding ratio obtained with a given outboard breeding blanket thickness -  $\text{Li}_2\text{O}$  breeder.

without the inboard breeding. Therefore, the inboard blanket for all the cases examined is composed of an identical composition of (90% PCA + 10%  $\text{H}_2\text{O}$ ) in the region with the 30-cm thickness.

It should not be concluded that it is certain that reactors can be designed without inboard breeding. Such a conclusion is not established at this time. In particular, more extensive, three-dimensional neutronics calculations give more pessimistic results for tritium breeding than the one-dimensional calculations appropriate for a survey study of this sort. It has been decided, however, to make the blanket model consistent with the calculations that have been used. This design results in constant inboard energy deposition rates of  $E_{14,06} = 20.20$  MeV per 14.06 MeV source neutron and  $E_{2,45} = 10.21$  MeV per 2.45-MeV source neutron. Figures 7 and 8 show the energy

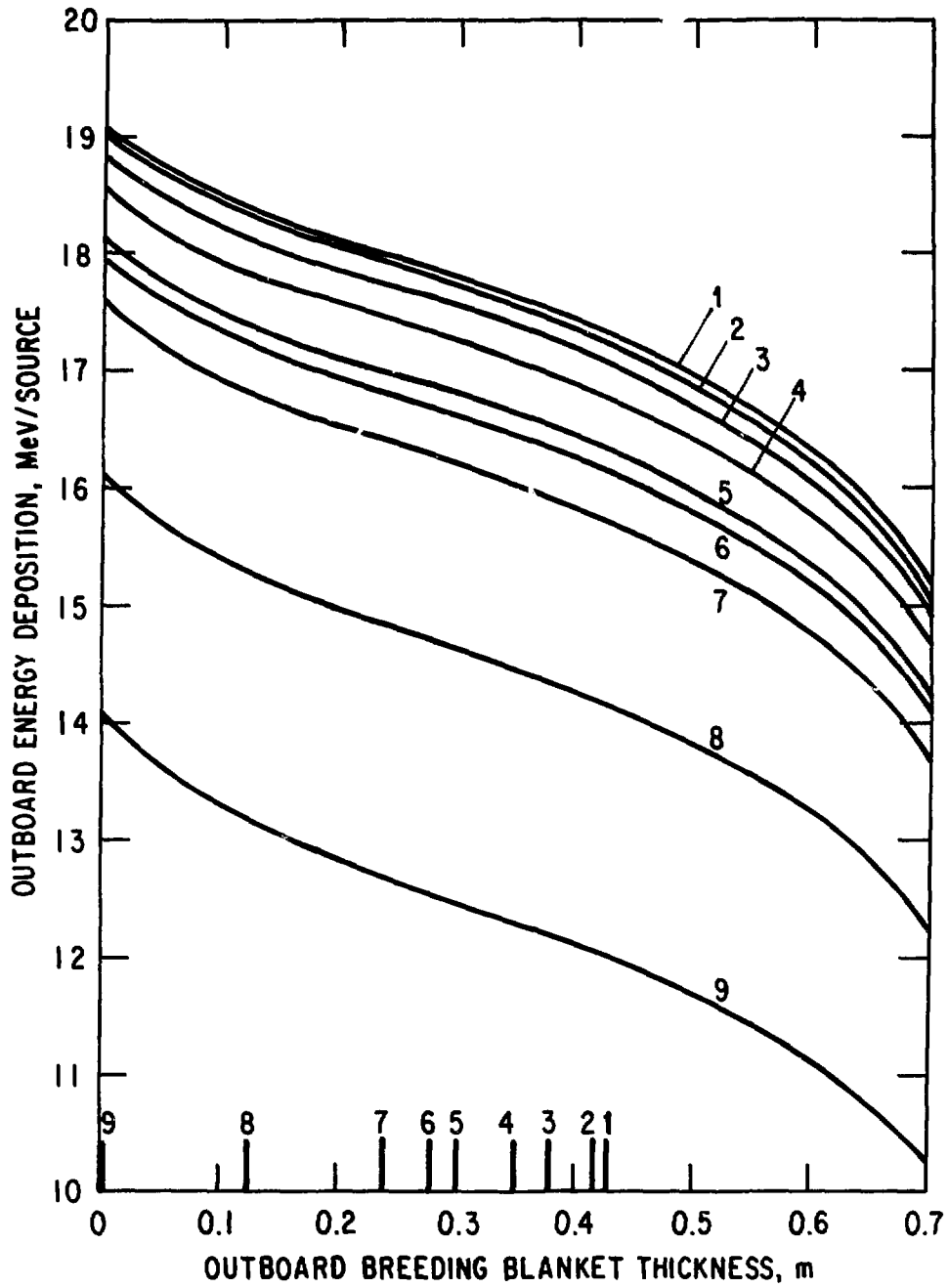


Fig. 7. Outboard energy deposition - liquid lithium breeder.

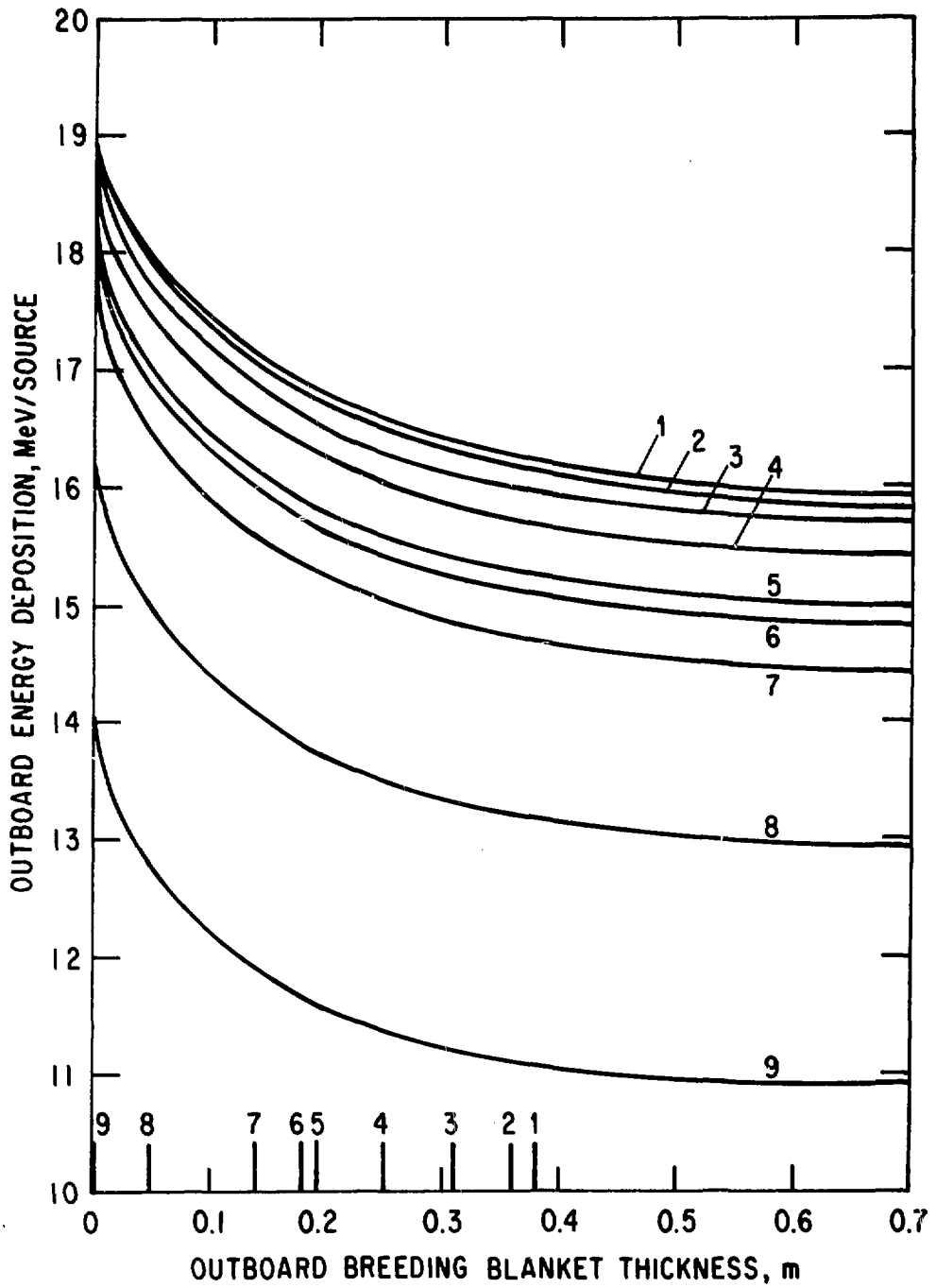


Fig. 8. Outboard energy deposition -  $\text{Li}_2\text{O}$  breeder.

deposition in the outer blanket/shield as a function of the thickness of the breeding zone part of the blanket for both blanket materials. Combining these results with the inboard energy deposition rates mentioned above, one can determine the respective energy multiplication factors,  $\epsilon_{14.06}$  and  $\epsilon_{2.45}$ , for the 14.06-MeV and 2.45-MeV sources.

#### D. Specific Reactor Designs

Reactor parameters have been calculated for nine specific designs with tritium concentrations ranging from unity to  $4.2 \times 10^{-3}$ , corresponding to TBR's from near unity to zero. For each of these designs two types of breeder blankets have been considered: liquid lithium (Li) and lithium oxide (Li<sub>2</sub>O). In order to have a consistent basis for comparison, all of the reactors have been taken to have: (1) a toroidal, rms beta of 10%; (2) a thermal power,  $P_T$ , of 4 Gwt; and (3) a first-wall heat load,  $P_{w,heat}$  (due to radiation and charged particles) of 1.0 MW/m<sup>2</sup>. The MHD equilibrium has been held constant except for simple scaling with  $R_0$  and  $B_{TFC}$ .<sup>12</sup> A scrapeoff thickness,  $\Delta_v$ , of 0.2 m has been assumed, and the electron temperature has been chosen as described in Sec. IV.B. Values of  $r_T$  have been chosen to adequately cover the three regions of interest described in that section. The net <sup>3</sup>He recycling coefficient,  $R_3$ , has been chosen to be 0.75 for  $r_T > 0.03$ . This is the value that is expected to occur because of recycling at the wall but with no reinjection of <sup>3</sup>He.<sup>1,2</sup> For  $r_T < 0.03$  all the <sup>3</sup>He that diffuses out is reinjected, corresponding to a net recycling coefficient,  $R_3$ , of unity. For the  $r_T = 0.03$  case both modes of operation are considered. These choices of  $R_3$  optimize the reactor designs except that the choice is not clear around the transition near  $r_T = 0.03$ .

The appropriate inside and outside blanket/shield thicknesses,  $\Delta_{BS}^i$  and  $\Delta_{BS}^o$ , and the neutron energy multiplications,  $\epsilon_{1406}$  and  $\epsilon_{245}$ , are calculated for each case as described in Sec. IV.C. These are shown in Fig. 9.

Table IV shows the specific values of  $r_T$  chosen for the nine designs along with other parameters which are determined by  $r_T$  and which do not depend on the size and magnetic field. The temperature from the model described in Sec. IV.B and the required tritium breeding ratio are shown along with a relative effectiveness parameter,  $\mathcal{R}$ , which is an indication of the loss in fusion power due to operation at lower values of  $r_T$ .

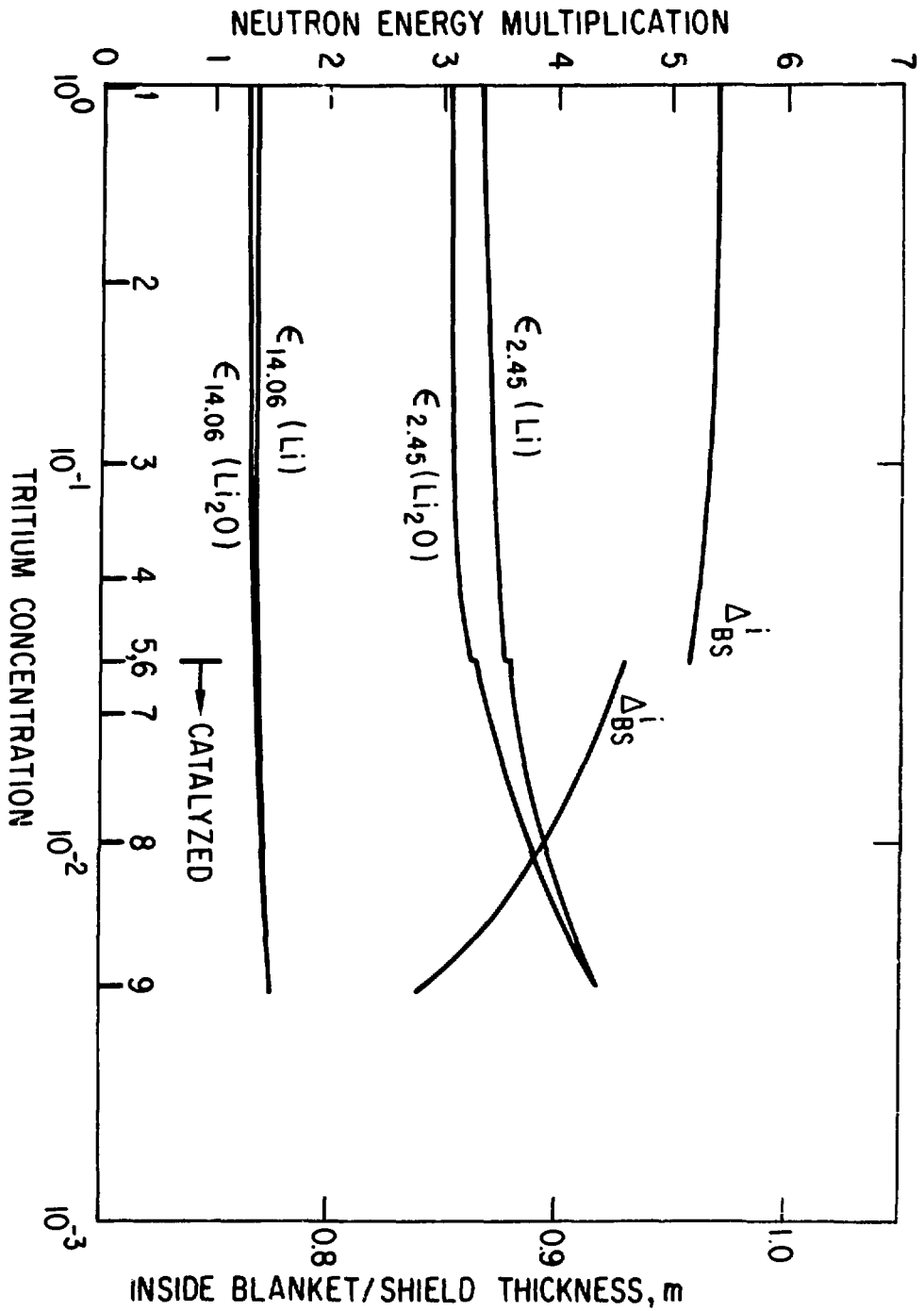


Fig. 9. Inboard blanket/shield thickness and energy multiplication.

TABLE IV

Tritium Concentrations Used for the Specific Designs and Related Quantities

Design	$r_T$	$R_3$	$T_e$ (keV)	TBR	$\mathcal{R}$	$\bar{n}_D \bar{T}_E$ ( $10^{20}$ s/m <sup>3</sup> )	$\bar{n}_P/\bar{n}_D$ (%)	$\bar{n}_3/\bar{n}_D$ (%)	$\bar{n}_4/\bar{n}_D$ (%)	$P_{w,neut}$ (MW/m <sup>3</sup> )
1	1.0	0.75	7.0	0.99	1.00	0.9	0.007	0.003	1.0	4.0
2	0.3	0.75	7.4	0.98	0.71	1.9	0.02	0.008	0.8	4.0
3	0.1	0.75	7.8	0.94	0.33	5.9	0.06	0.03	0.9	3.9
4	0.05	0.75	9.8	0.89	0.18	11.1	0.18	0.08	1.3	3.7
5	0.03	0.75	13.0	0.81	0.10	17.7	0.49	0.21	1.9	3.5
6	0.03	1.00	17.5	0.78	0.05	13.1	1.2	18.	2.2	2.2
7	0.022	1.00	18.7	0.70	0.04	16.0	1.7	16.	2.2	1.8
8	0.01	1.00	21.9	0.40	0.02	21.9	2.9	14.	2.0	1.1
9	0.0042	1.00	24.0	0.	0.01	27.1	4.1	12.	1.7	0.6

The quantity,  $\mathcal{R}$ , is defined as follows. First, an effective reactivity, " $\langle\sigma v\rangle$ ", is defined from:

$$P_F = \bar{n}_D^2 \langle\sigma v\rangle E_{DT} V_p, \quad (2)$$

where  $P_F$  is the fusion power from the plasma (not including blanket neutron energy multiplication),  $\bar{n}_D$  is the average deuteron density,  $E_{DT}$  is the energy release (17.6 MeV) for the D-T reaction, and  $V_p$  is the plasma volume. An effective temperature,  $\bar{T}$ , is defined from:

$$\beta_t \equiv \frac{2\bar{\mu}p}{B_{to}^2} = \frac{\bar{\mu} \bar{n}_D k \bar{T}}{B_{to}^2}, \quad (3)$$

where  $\bar{p}$  is the average plasma pressure, and  $B_{to}$  is the magnetic field in the center of the plasma. The quantity  $\bar{T}$  contains the effects of pressure of all the thermal and superthermal particles. The fusion power is then given by:

$$P_F = \frac{B_{to}^4 \beta_t^2 V_p \langle\sigma v\rangle E_{DT}}{\mu^2 k^2 \bar{T}^2}, \quad (4)$$

and the relative effectiveness,  $\mathcal{R}$ , is the value of " $\langle\sigma v\rangle/\bar{T}^2$ " relative to its value for the D-T reactor:

$$\mathcal{R} = \frac{\langle\sigma v\rangle/\bar{T}^2}{\left[ \frac{\langle\sigma v\rangle}{\bar{T}^2} \right]_{DT}}. \quad (5)$$

The importance of  $\mathcal{R}$  is that  $P_F$  is proportional to  $\beta_{to}^2 B_{to}^2 V_p \mathcal{R}$ , and  $\mathcal{R}$  represents the loss in fusion power that results from lowered values of  $r_T$ . The loss occurs because of reduced reactivities, increased temperatures, and increased amounts of fuel other than deuterium and tritium. From Table III, for example it can be seen that in some sense a Cat-D plasma is only ~1% as effective for power production as a D-T plasma. Some of the loss indicated by  $\mathcal{R}$  can be made up by thinner blankets and greater neutron energy multiplication.

Also shown in Table IV are the electron energy confinement parameter,  $\bar{n}_D \tau_E$ , the relative concentrations of the plasma components, and the neutron wall load. The value of  $\bar{n}_D \tau_E$  required for ignition increases rapidly as  $r_T$  is decreased, but the confinement required is still less than that predicted by

empirical scaling<sup>15</sup> for all the reactor designs considered. The amounts of P and <sup>3</sup>He are nearly proportional to  $\bar{n}_D r_T$  and also increase as  $r_T$  decreases. The cases with  $R_3 = 1.0$  have substantially more <sup>3</sup>He. Finally, it can be seen that the neutron wall load and hence the total wall load are strongly reduced as  $r_T$  decreases. In general, for a reactor that is first-wall heat-load limited, less power is produced when there are proportionately more charged particles, so that a lower neutron fraction is a disadvantage.

After the above parameters are determined, the required major radius,  $R_0$ , and the required peak toroidal field,  $B_{TFC}$ , which give the desired thermal power and wall load can be calculated. These two parameters most obviously distinguish the designs from each other. The major radius is shown in Fig. 10 and the peak field, in Fig. 11 for both types of breeder material. It can be seen there is little difference between the two types of breeder material, the lithium case being slightly smaller but having slightly higher field.

Also shown in Figs. 10 and 11 are the values of the major radius and field if all of the <sup>3</sup>He were recycled for all values of the tritium concentration. It can be seen that recycling the <sup>3</sup>He is disadvantageous, resulting in both larger size and higher field, provided  $\bar{r}_T > \sim 0.04$ . The disadvantage of the <sup>3</sup>He as ash outweighs its merit as a fuel for these cases. On the other hand if the <sup>3</sup>He is not recycled, operation below  $r_T \sim 0.02$  is not possible. There is not enough fusion heat produced to satisfy the power balance for the electrons. Adding <sup>3</sup>He is effective for heating since the D-<sup>3</sup>He reaction products are both charged and energetic (18.34 MeV). In general, catalyzation is necessary below  $r_T$  on the order of one percent. The exact value of  $r_T$  depends on such factors as impurity content in the plasma, fraction of cyclotron radiation reflected, and the diffusion and recycling rates of all of the particles.

It can be seen from Fig. 10 that the reactor size, which is the predominant determinant of the reactor cost, is relatively insensitive to tritium concentration until catalyzation is necessary. It then increases rapidly. The major effect of operating at reduced tritium levels is an increase in the required toroidal field as long as catalyzation is not necessary.

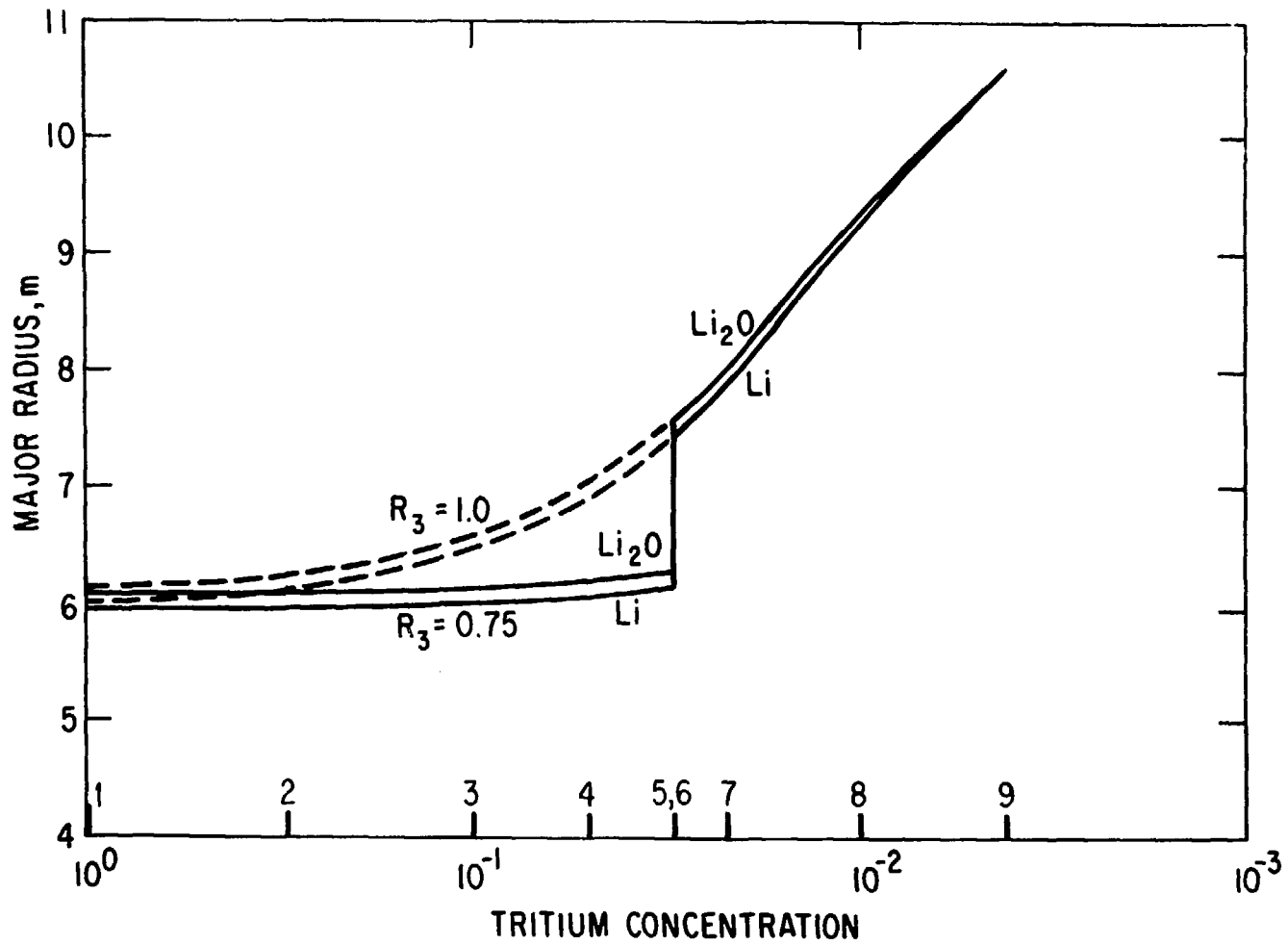


Fig. 10. Major radius as a function of tritium concentration for fixed thermal power and first-wall heat load.

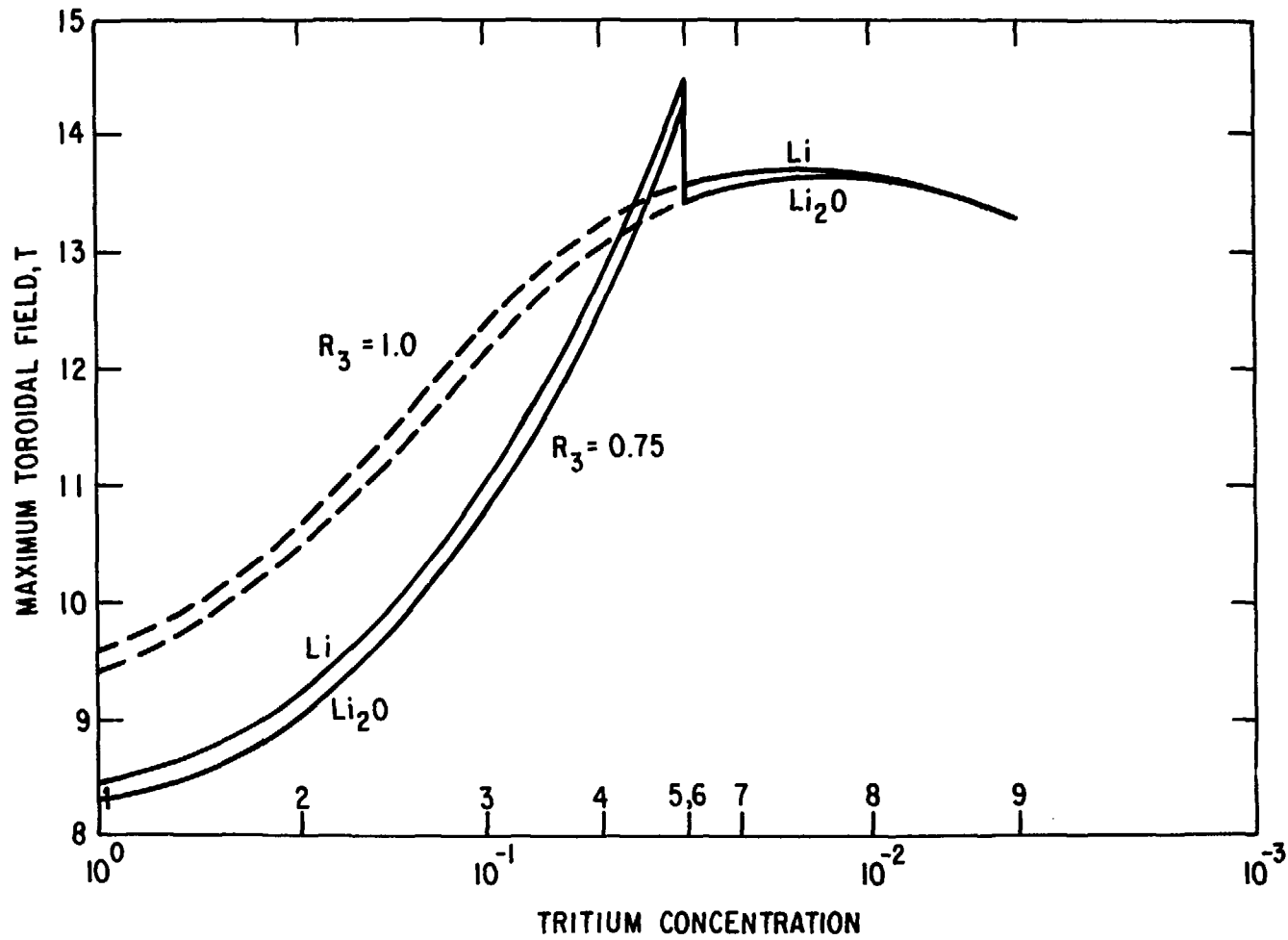


Fig. 11. Peak toroidal field as a function of tritium concentration for fixed thermal power and fixed wall heat load.

## V. TRITIUM CONSIDERATIONS

The major advantage of WILDCAT over STARFIRE was its greatly reduced tritium inventories and throughputs, nearly two orders of magnitude less than the STARFIRE values. Figure 12 shows how the amounts of tritium that are being transported through the reactor vary as a function of tritium concentration. In this figure the plasma exhaust is the amount of tritium leaving the plasma (the difference between the diffusion rate and the reflection rate). The tritium burnup is the total burnup rate of tritium via the D-T reaction including superthermal fusions. This tritium comes from tritium production in the plasma via the  $D + D \rightarrow p + T$  reaction and from fueling of tritium. The fuel throughput consists of the bred tritium and the reinjection of tritium that has diffused out of the plasma and not been reflected at the wall.

It can be seen that the tritium burnup rate remains relatively constant, falling off somewhat after catalyzation is necessary. As a consequence, for all of these reactors (and as was true for WILDCAT) the bulk of the power still comes from the D-T reaction. The tritium production rate in the plasma, which is negligible for a D-T reactor, increases as the D-D reactions become more important, eventually equaling the burnup rate at the value of  $r_T$  that can be supported without breeding tritium. The fuel throughput and plasma exhaust, the tritium which has to be handled in the plant, decrease sharply and steadily as  $r_T$  decreases.

One can define two categories of tritium stored in the reactor. The vulnerable inventory consists of tritium which is most subject to accidental release. For this paper this vulnerable tritium is assumed to consist of (1) 5 h of exhaust in the vacuum pumps; (2) 1 h of fueling plus 1 g holdup in the fueling system; and (3) 12 h of residence time in the blanket processing system. The nonvulnerable inventory, which is not readily released, consists of (1) 2 days of burnup (plus 2 days of exhaust for the catalyzed cases) for fueling; (2) 1 day of residence time in the blanket for lithium and 10 days for  $Li_2O$ ; and (3) 3 h of residence time in the fuel processing system. This model reproduces the STARFIRE and WILDCAT values reasonably well, although the nonvulnerable holdup in the blanket was assumed larger at the time STARFIRE was designed and more frequent valve replacement was utilized to reduce the vulnerable inventory. It can be noted that even though the blanket inventory

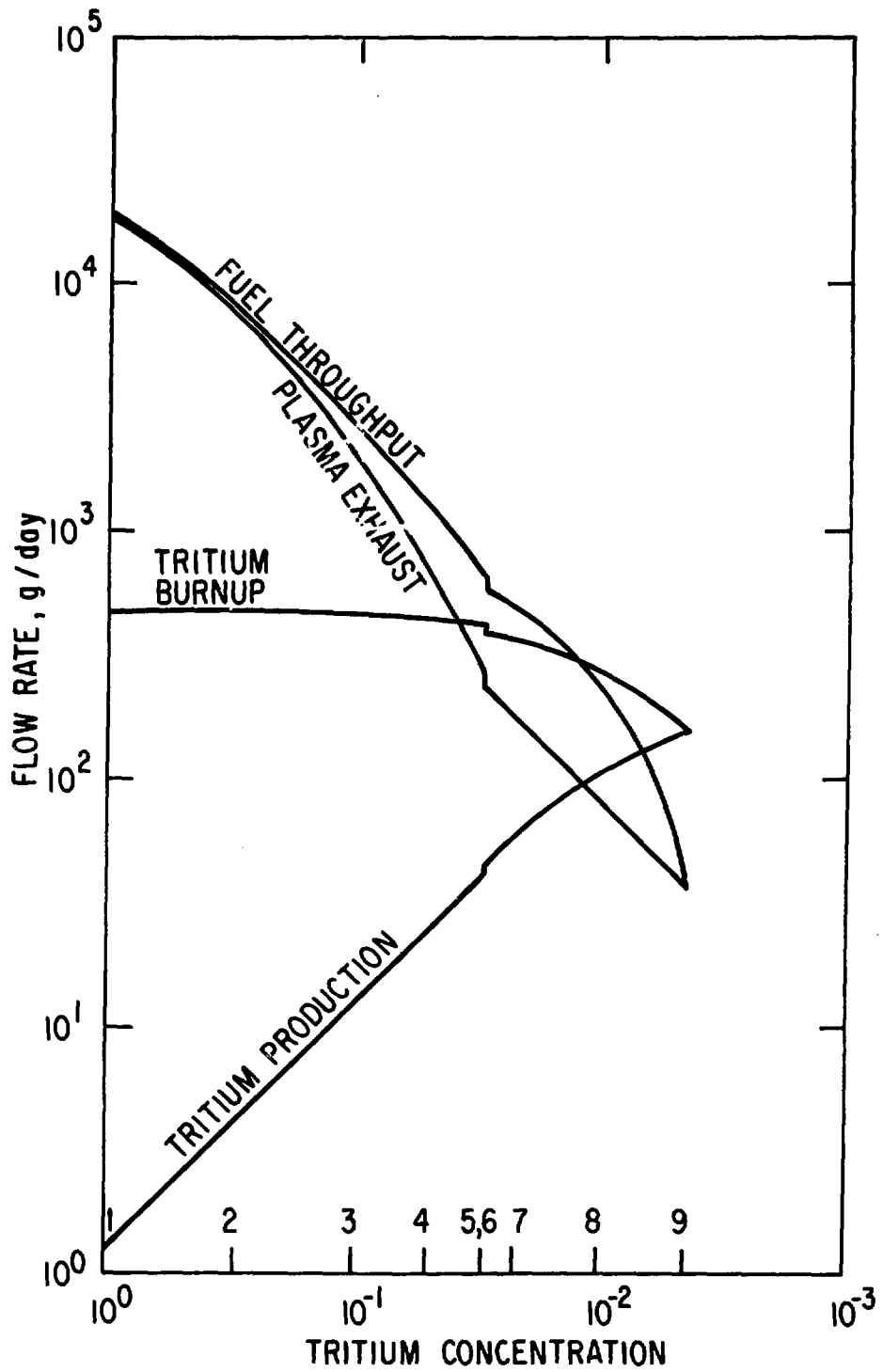


Fig. 12. Rates of tritium burnup, production, exhaust, and fueling.

is larger if the residence time in the blanket is longer, the inventory is less vulnerable. The vulnerable and nonvulnerable inventories are shown in Fig. 13. They also decrease sharply and steadily with  $r_T$ .

## VI. COSTING

It is difficult to make unequivocal statements concerning fusion reactor costing at this stage in the development of fusion, because there are so many unknown factors. On the other hand, almost all design choices are ultimately made on the basis of cost effectiveness. It is hence important to think about the impact of costing on reactor design, even though the conclusions may not be hard and fast and will almost certainly change as the study of fusion progresses.

The cost model used in this study has been designed to use the costing assumptions and procedures that were used for STARFIRE and WILDCAT. For comparison purposes the costs are given in constant, 1980 dollars, the same as presented in those studies. A detailed description of the guidelines, procedures, and breakdown of the cost accounts is given in Refs. 1 and 2. A more extensive description of the cost model is given in Ref. 16.

For the purposes of this study it is desirable to have a parametric cost model that is valid for a wide range of reactors. The cost model used is based on simple scaling formulas for each cost account with STARFIRE taken as the base point. Scaling laws have been found, however, which also reproduce WILDCAT. Having a model which is normalized to these two substantially different cases should insure a good degree of validity for a wide range of reactors with similar types of reactor subsystems.

The basic model matches STARFIRE identically and matches most cost accounts of WILDCAT to better than ten percent. The only less than satisfactory match is for Account 22.01.07, Power Supplies, Switching, and Energy Storage, which is calculated to be nearly twice the actual WILDCAT value. The discrepancy is due to a substantially more cost-effective design in WILDCAT; in particular the use of two power supplies for different parts of the EF current ramp and longer startup and shutdown times. Since these features represent real improvements, a modified model is used in this paper with the EF power supplies scaled from WILDCAT.

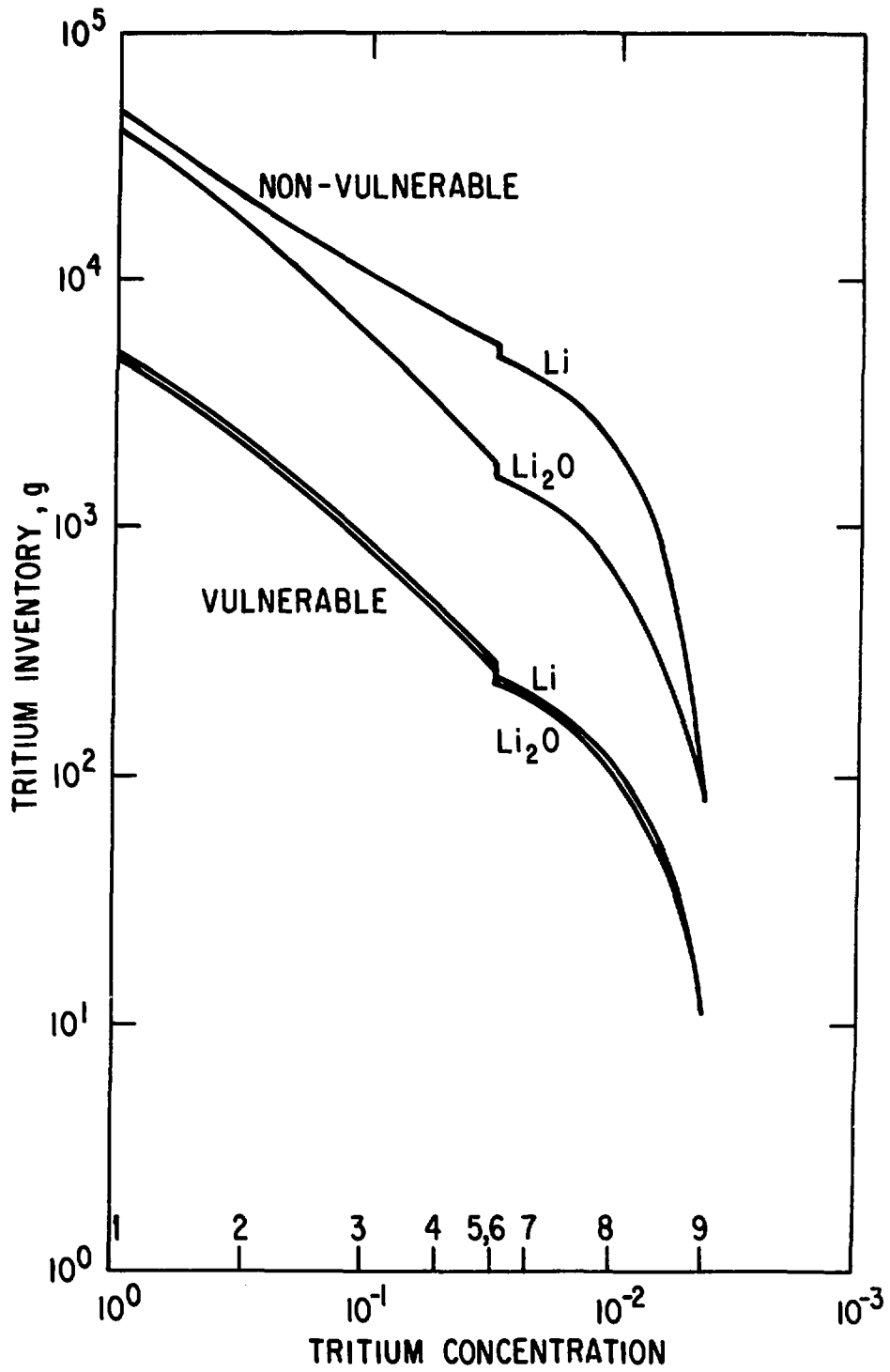


Fig. 13. Tritium inventories.

The RF heating and current-drive methods are different for STARFIRE and WILDCAT and both are also different from the REB current-drive method in this report. Accordingly the costing for this system is scaled to DEMO<sup>7</sup> for the REB system.

A comparison of the basic and modified cost models with the actual STARFIRE and WILDCAT costing is shown in Table V for the interesting cost accounts. The total costs and cost of electricity (COE) are matched to about one percent or better, well within the accuracy of the actual costing.

The costs for the reactor designs considered in this paper are shown in Fig. 14 for the lithium case. The  $\text{Li}_2\text{O}$  case is little different. The toroidal coils are sized by allowing 1 m between the outer shield and the magnets. Toroidal field ripple requirements have been ignored. Both the total plant cost and the cost of the reactor alone are shown in Fig. 14 as well as the cost of electricity. The costs do not increase rapidly as the tritium concentration decreases until catalyzation becomes necessary. After that point the costs begin to increase rather sharply. The balance-of-plant costs remain relatively constant, so that the higher cost is driven by the larger-sized and higher-field reactor.

Because of the assumption of higher beta, the total plant cost and the cost of electricity for the D-T reactor (Design 1) are less than for STARFIRE. The total plant cost of the D-D reactor (Design 9) is higher than that of WILDCAT because the assumed beta is lower. The cost of electricity for the D-D reactor is, however, lower than for WILDCAT. The reason is that the net electric power has increased more than the cost. The cost of electricity, in general, decreases as the thermal power is increased, and the D-D reactor in this study has a thermal power of 4 GW compared to 3 GW for WILDCAT.

From the cost curves it would appear that a catalyzed reactor is always more costly than an uncatalyzed reactor (as long as the uncatalyzed mode is possible). In addition, the use of a lithium or lithium oxide blanket seems to make little difference in the cost.

The overall conclusion is that it would appear that there is little cost penalty for operating in a tritium-depleted mode down to a tritium concentration of approximately 0.1 or TBR of approximately 90%. This conclusion is a result of two facts: (1) under the restrictions of this study the major

TABLE V

## Costing Model Results for STARFIRE and WILDCAT.

Costs are in 1980 M\$ unless noted.

Account	Title	Basic Model		Modified Model		WILDCAT Actual
		STARFIRE <sup>a</sup>	WILDCAT	STARFIRE	WILDCAT	
20.	Land	3.30	3.30	3.30	3.30	3.30
21.	Structures	346.58	346.58	346.58	346.58	346.59
22.	Reactor equipment	968.62	1522.14	941.67	1490.13	1496.63
22.01.01	Blanket/first wall	82.36	148.41	82.36	148.41	132.23
22.01.02	Shield	186.07	334.21	186.07	334.21	352.50
22.01.03	Magnets	171.57	342.01	171.57	342.01	352.66
22.01.04	RF heating/current drive	33.49	34.88	33.49	34.88	34.88
22.01.05	Structure	52.74	121.02	52.74	121.02	115.13
22.01.06	Vacuum	4.86	11.50	4.86	11.50	8.68
22.01.07	Power supplies	52.90	62.06	29.86	34.70	32.20
22.01.08	Impurity control	2.45	3.07	2.45	3.07	3.07
22.01.09	ECRH breakdown	2.82	9.45	2.82	9.45	15.60
23.	Turbine equipment	249.68	205.76	249.68	205.76	215.38
24.	Electric equipment	117.28	110.95	227.29	110.95	111.08
25.	Miscellaneous equipment	40.77	40.77	40.77	40.77	39.66
26.	Special materials	0.25	0.25	0.25	0.25	0.25
90.	Total direct cost	1726.48	2229.75	1699.54	2197.74	2212.89
99.	Total cost	2400.27	3099.95	2362.82	3055.45	3076.51
	Net electric, MW(electrical)	1202.	803.	1202.	803.	812.
	COE, mills/kW(electrical)	35.1	63.5	34.6	62.7	62.8

<sup>a</sup>These are the same as the actual STARFIRE figures.

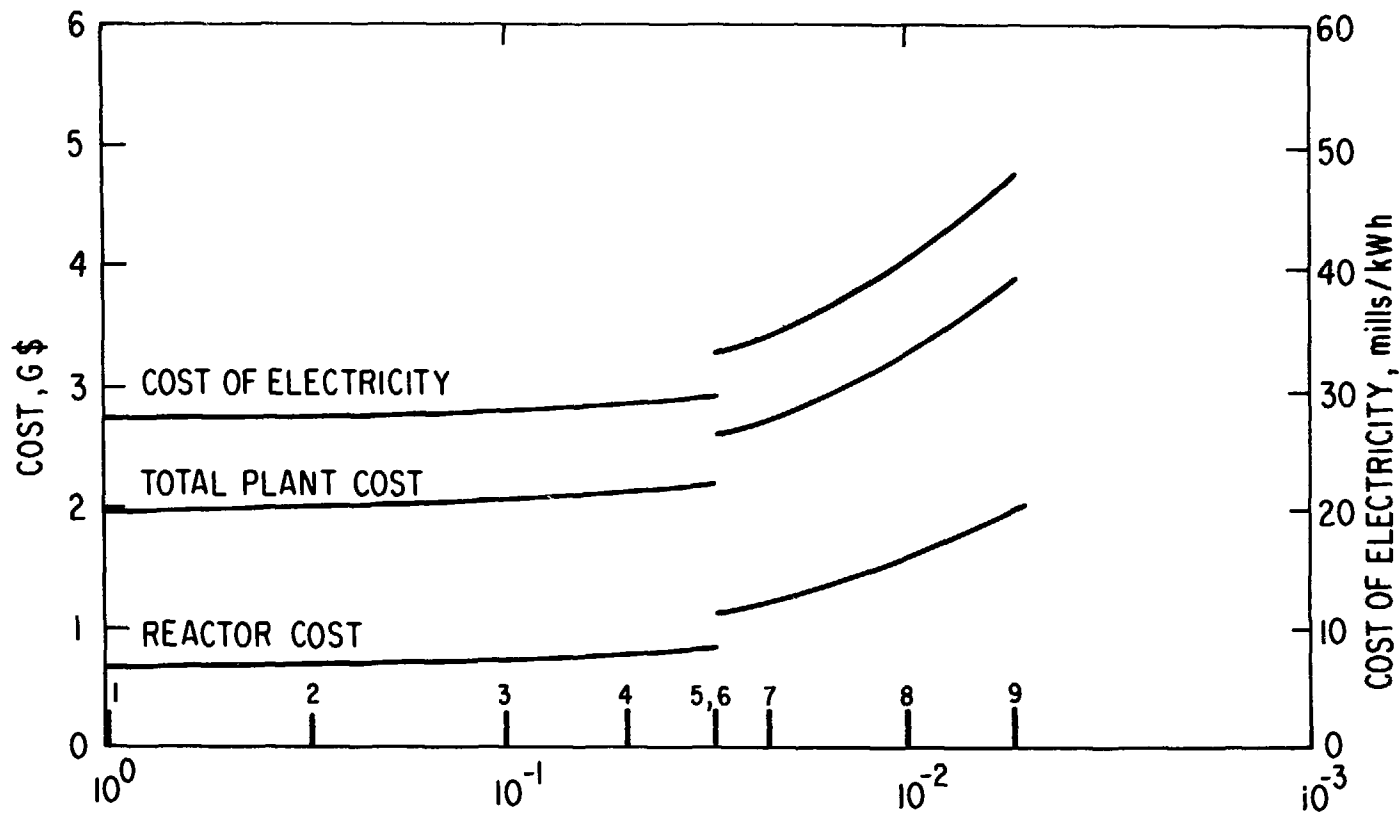


Fig. 14. Cost analysis.

effect of a decrease in  $r_T$  near  $r_T = 1$  is an increase in the toroidal field; and (2) the cost model does not show a strong dependence on toroidal field, consistent with the STARFIRE/WILDCAT costing, on which a credible amount of effort has been spent.

Because of the strong dependence of the reactor power on the magnetic field in the plasma, it seems to be a general rule that factors which tend to degrade the power density (such as reduced tritium fueling) can often be compensated for by relatively small changes in the peak toroidal field. (Similarly, increases in the power density, for example by the use of polarized fuels,<sup>17</sup> only lead to relatively minor decreases in the peak field.) Such increases would be cost effective as long as the costs of increased magnetic field do not increase too quickly with field.

It is not possible to determine all of the cost implications of higher field in a study of this scope. It can be noted, however, that it would take a substantially stronger dependence of cost on magnetic field to seriously invalidate the above conclusion. The reason is that the affected costs do not dominate the overall cost as does, for example, a change in the major radius. In addition, even for  $r_T = 0.05$  or TBR = 89%, the field is 12.8 T. This value is not so far from the STARFIRE value to expect the costing to be invalid.

On the other hand, the assumption of very efficient, REB, current drive may cause the impact of the higher plasma currents associated with the higher fields to be underestimated. Further, all of the problems associated with higher field are difficult to quantify, and may not be adequately represented in the costing. Impact on the plant availability, for example, can be very costly.

It should also be noted that this study has not adequately dealt with the problem of reduced breeding effectiveness, for example by keeping the same blanket and examining varying amounts of tritium production. This issue is treated in Ref. 18.

## VII. SUMMARY AND CONCLUSIONS

A sequence of reactors covering the range from full tritium breeding to no tritium breeding has been presented. Apart from the plasma tritium concentration these reactors have a consistent design basis. In particular they all

have a plasma beta of 10%, a thermal power output of 4 GW, and a heat wall load of 1 MW/m<sup>2</sup>. They are all steady-state tokamaks with an efficient, relativistic-electron-beam current drive.

The optimum operating temperature, defined as the temperature at which the power density peaks or a few keV above the minimum temperature for ignition whichever is larger, has been found as a function of tritium concentration. This temperature increases from 7 keV for full D-T operation to 24 keV when there is no tritium breeding. These average temperatures depend on the shape of the temperature profile and would be different if different profiles were chosen. The peak temperature would remain relatively constant.

Reinjection of the <sup>3</sup>He produced in the plasma is deleterious for high tritium concentrations, but is necessary if ignition is to be obtained below a tritium concentration on the order of 10<sup>-2</sup> corresponding to breeding ratios below ~50%.

For operation with tritium concentrations above the point where reinjection of the <sup>3</sup>He is necessary, the inner blanket/shield thickness is relatively constant, and no major increase in the neutron energy multiplication is seen. Below  $r_T \sim 0.03$  the inner blanket/shield thickness decreases, and a strong enhancement of the 2.45-MeV neutron energy multiplication and a lesser enhancement of the 14.06-MeV neutron energy multiplication begins to occur. These improvements do not, however, make up for the reduced effectiveness,  $\mathcal{R}$ , of the fusion reactions.

Since the plasma beta, the thermal power, and the heat wall load are fixed, the major characteristics distinguishing the reactors with different tritium concentrations are the size and magnetic field. The size stays roughly constant (near 6 m) down to the point where reinjection of the <sup>3</sup>He becomes necessary, then increases rapidly. The magnetic field increases steadily until the point where reinjection becomes necessary then remains relatively constant (near 14 T). The actual values of the size and field depend, of course, on the value of the plasma beta.

The tritium inventories and throughputs decrease steadily as the tritium concentration is decreased, approximately proportionately to  $r_T$ . These reduced amounts of tritium are the major benefit of operation at low values of  $r_T$ .

The cost of the reactor, the total plant cost, and the cost of electricity increase slowly until the point where reinjection of the  $^3\text{He}$  is necessary, then begin to increase more rapidly. The total cost of the nonbreeding plant is about twice that of the full D-T plant; the cost of the reactor alone is about three times as large; and the cost of electricity is a little more than twice as large.

There appear to be three distinct regions of interest as far as tritium concentrations or tritium breeding ratio is concerned. For  $r_T \geq 0.1$ , which corresponds to  $\text{TBR} \geq 94\%$ , the reactors are similar to a full D-T reactor. The  $^3\text{He}$  would not be reinjected; the maximum in the power density is above the minimum temperature for ignition; the size is nearly constant although the magnetic field is increasing; and the reactor cost as well as the cost of energy, which depend most strongly on size, do not vary greatly. This could be considered the region of slightly-deteriorated, D-T operation.

For  $r_T \leq 0.01$ , which corresponds to  $\text{TBR} \leq 40\%$ , the reactors are more similar to a D-D reactor such as WILDCAT. Reinjection of  $^3\text{He}$  is necessary; the maximum in the power density falls below the minimum temperature for ignition, which is relatively high; the size is increasing strongly while the magnetic field is already large; and both the cost and cost of energy are increasing rapidly. This region is much less attractive from most points of view, although it does have the benefit of reduced tritium inventories and throughputs. The deteriorated operation is a result of the fact that the effectiveness of the fusion reactions has become less than 2% of that of a full D-T plasma.

The intermediate region with  $0.1 \leq r_T \leq 0.01$ , corresponding to tritium breeding ratios in the range of 40-90%, is a transition region. Reinjection of  $^3\text{He}$  is becoming necessary, the operating temperature is rising, the size is increasing, the magnetic field is already high, and the costs are beginning to increase strongly. The effectiveness of the fusion reactions is less than one-third that of a full D-T plasma, and is beginning to decrease rapidly. In addition, the margin for ignition is beginning to decrease, and the required confinement is already nearly an order-of-magnitude above that of a full D-T reactor.

There hence appears to be incentive to provide sufficient tritium breeding to avoid penetrating too far into the transition region, but perhaps les-

ser incentive to achieve full D-T operation. Less than full tritium breeding, however, implies increased technology requirements, especially in connection with higher magnetic fields and the attendant higher stresses and with higher currents in the plasma and poloidal coils.

#### ACKNOWLEDGMENTS

The authors are indebted to D. A. Ehst for discussions about rf current drive, to P. Finn and R. Clemmer for discussions and help regarding the tritium inventory model, to D. Baxter for making available the Science Applications, Inc., D-D costing code, which was very helpful in developing the costing algorithm used in this study, and to C. C. Baker for discussions and several important critical comments. The author is also grateful to Cyrilla Hytry for the preparation of this report.

**REFERENCES**

1. C. C. BAKER et al., "STARFIRE - A Commercial Tokamak Fusion Power Plant Study," ANL/FPP-80-1, Argonne National Laboratory (1980).
2. K. EVANS, JR., et al., WILDCAT: A Catalyzed D-D Tokamak Reactor, ANL/FPP/TM-150 (1981).
3. E. GREENSPAN and G. MILEY, Nucl. Technol./Fusion 2, 590 (1982).
4. R. W. CONN, et al., "SATYR Studies of a D-D Fueled Axisymmetric Tandem Mirror Reactor," PPG-576, Univ. California-Los Angeles (1981).
5. D. COHN, Massachusetts Institute of Technology, personal communication (1982).
6. See Ref. 2 for the analytical form of the plasma boundary and exact definitions of the other MHD parameters.
7. M. A. ABDU, et al., "A Demonstration Tokamak Power Plant Study (DEMO)," ANL/FPP-82-i (1982).
8. L. A. TURNER and M. A. ABDU, "Computational Model for Superconducting Toroidal Field Magnets for a Tokamak Reactor," ANL/FPP/TM-88, Argonne National Laboratory (1977).
9. "ANISN-ORNL: Multigroup One-Dimensional Discrete Ordinates Transport Code with Anisotropic Scattering," ORNL/RSIC-254, Oak Ridge National Laboratory (1973).
10. R. W. ROSSIN, et al., "VITAMIN-C: The CTR Processed Multigroup Cross Section Library for Neutronics Studies," ORNL/RSIC-37 (ENDF-296), Oak Ridge National Laboratory (1980).
11. Y. GOHAR and M. ABDU, "MACKLIB-IV: A Library of Nuclear Response Functions Generated with the MACK-IV Computer Program from ENDF/B-IV," ANL/FPP/TM-106, Argonne National Laboratory (1978).
12. K. EVANS, JR., et al., "D-D Tokamak Reactor Studies," ANL/FPP/TM-138, Argonne National Laboratory (1980).
13. E. GREENSPAN and G. MILEY, Nucl. Technol./Fusion 2, 43 (1982).
14. K. EVANS, JR., High  $\beta_t$  Equilibria in Tokamaks, ANL/FPP/TM-98, Argonne National Laboratory (1977).
15. D. R. COHN, R. R. PARKER and D. L. JASSBY, Nucl. Fusion 16, 31 (1976); and D. L. JASSBY, D. R. COHN and R. R. PARKER, Nucl. Fusion 16, 1045 (1976).
16. K. EVANS, JR., "A Tokamak Reactor Cost Model Based on STARFIRE/WILDCAT Costing," ANL/FPP/TM-168 (1983) Argonne National Laboratory.

17. R. M. KULSRUD, H. P. FURTH, E. J. VALEO, and M. GOLDBABER, "Fusion Reactor Plasma with Polarized Nuclei," PPPL-1912, Princeton Plasma Physics Laboratory (1982).
18. J. GILLIGAN, K. EVANS, and J. JUNG, "The Effective Cost of Tritium for Tokamak Fusion Power Reactors with Reduced Tritium Breeding Ratios," Proc. 5th Top. Mtg. on The Technology of Fusion Energy, Knoxville, TN, April 16-28, 1983; Nucl. Technol./Fusion (to be issued).

Distribution for ANL/FPP/TM-169

Internal:

M. Abdou	D. Gruen	R. Mattas
C. Baker	A. Hassanein	B. Misra
E. Beckjord	C. Johnson	R. Nygren
C. Boley	J. Jung (5)	J. Roberts
J. Brooks	M. Kaminsky	D. Smith
F. Cafasso	S. Kim	L. Turner
Y. Cha	Y-K. Kim	R. Wehrle
R. Clemmer	R. Kustom	ANL Patent Dept.
D. Ehst	R. Lari	FP Program (25)
K. Evans (5)	L. LeSage	ANL Contract File
P. Finn	B. Loomis	ANL Libraries (2)
Y. Gohar	S. Majumdar	TIS Files (6)

External:

DOE-TIC, for distribution per UC-20, 20d (128)  
Manager, Chicago Operations Office, DOE  
Special Committee for the Fusion Program:  
S. Baron, Burns & Roe, Inc., Oradell, NJ  
H. K. Forsen, Exxon Nuclear Company, Inc., Bellevue, WA  
M. J. Lubin, Standard Oil Company of Ohio, Warrensville Heights, O  
G. H. Miley, University of Illinois, Urbana  
P. J. Reardon, Princeton University  
D. Steiner, Rensselaer Polytechnic Institute  
K. R. Symon, University of Wisconsin-Madison  
K. Thomassen, Lawrence Livermore National Laboratory  
R. Aamodt, Science Applications, Inc., La Jolla, CA  
W. Allen, Bechtel National, Inc., San Francisco, CA  
N. Amherd, Electric Power Research Institute, Palo Alto, CA  
D. J. Anthony, General Electric Company, Schenectady, NY  
R. E. Aronstein, Bechtel National, Inc., San Francisco, CA  
C. Ashworth, Pacific Gas and Electric Company, San Francisco, CA  
K. M. Barry, The Ralph M. Parsons Company, Pasadena, CA  
D. C. Baxter, Science Applications, Inc., La Jolla, CA  
L. A. Berry, Oak Ridge National Laboratory, Oak Ridge, TN  
S. L. Bogart, Science Applications, Inc., La Jolla, CA  
J. Boles, Laser Energetics Laboratory, Rochester, NY  
A. E. Bolon, University of Missouri, Rolla, MO  
R. Bonomo, University of Wisconsin, Madison, WI  
A. Boozer, Princeton Plasma Physics Laboratory, Princeton, NJ  
R. Botwin, Grumman Aerospace Corporation, Bethpage, NY  
M. H. Brennan, Sydney University, Sydney, Australia  
L. Bromberg, Massachusetts Institute of Technology, Cambridge, MA  
S. Burnett, GA Technologies, San Diego, CA  
R. N. Byrne, Science Applications Institute, La Jolla, CA  
G. Carlson, Lawrence Livermore National Laboratory, Livermore, CA  
G. Casini, Commission of the European Community, Ispra, Italy  
A. Chachich, Rensselaer Polytechnic Institute, Troy, NY

F. F. Chen, University of California-Los Angeles  
R. Cherdak, Burns & Roe, Oradell, NY  
B. Clancy, Lucas Heights Research Laboratory, Sutherland, Australia  
D. Cohn, Massachusetts Institute of Technology, Cambridge, MA  
R. Conn, University of California-Los Angeles  
B. Coppi, Massachusetts Institute of Technology, Cambridge, MA  
J. Crocker, EG&G Idaho, Inc., Idaho Falls, ID  
A. Dabiri, Science Applications, Inc., La Jolla, CA  
R. Davidson, Massachusetts Institute of Technology, Cambridge, MA  
J. Davis, McDonnell Douglas Astronautics Company, St. Louis, MO  
S. Dean, Fusion Power Associates, Gaithersburg, MD  
D. DeFreece, McDonnell Douglas Astronautics Company, St. Louis, MO  
D. Dingee, Battelle Pacific Northwest Laboratory, Richland, WA  
D. Dobrott, Science Applications, Inc., La Jolla, CA  
H. Dreicer, Los Alamos National Laboratory, Los Alamos, NM  
T. K. Fowler, Lawrence Livermore National Laboratory, Livermore, CA  
H. Furth, Princeton Plasma Physics Laboratory, Princeton, NJ  
J. Gialambos, University of Illinois, Urbana, IL  
J. Gilligan, University of Illinois, Urbana, IL  
J. Glancy, Science Applications, Inc., La Jolla, CA  
E. Greenspan, Nuclear Research Centre-Negev, IAEC, Beer-Sheva, Israel  
W. Grossmann, New York University, New York, NY  
W. K. Hagan, Science Applications, Inc., La Jolla, CA  
R. L. Hagenson, Los Alamos National Laboratory, Los Alamos, NM  
J. Hancox, Culham Laboratory, UKAEA, Abingdon, Oxfordshire, England  
R. Hawryluk, Princeton Plasma Physics Laboratory, Princeton, NJ  
R. L. Hirsch, Exxon Research & Engineering Company, Florham Park, NJ  
J. Holmes, Hanford Engineering Development Laboratory, Richland, WA  
W. Houlberg, Oak Ridge National Laboratory, Oak Ridge, TN  
D. Jassby, Plasma Physics Laboratory, Princeton, NJ  
E. A. Jackson, University of Illinois, Urbana, IL  
T. Kammash, University of Michigan, Ann Arbor, MI  
D. Kerst, University of Wisconsin, Madison, WI  
A. Knoblock, Max-Planck Institute fur Plasmaphysik, Garching, West Germany  
J. Kokozenski, The Ralph M. Parsons Company, Pasadena, CA  
R. A. Krakowski, Los Alamos National Laboratory, Los Alamos, NM  
D. Kummer, McDonnell Douglas Astronautics Company, St. Louis, MO  
T. Latham, United Technologies Research Center, East Hartford, CT  
K. J. Lee, University of Wisconsin, Madison, WI  
L. M. Lidsky, Massachusetts Institute of Technology, Cambridge, MA  
F. J. Loeffler, Purdue University, West Lafayette, IN  
T. Luzzi, Grumman Aerospace Corporation, Bethpage, NY  
J. F. Lyon, Oak Ridge National Laboratory, Oak Ridge, TN  
D. Lyster, Cornell University, Ithaca, NY  
D. G. McAlees, Exxon Nuclear Company, Bellevue, WA  
J. McBride, Science Applications, Inc., LaJolla, CA  
R. T. McGrath, Pennsylvania State University, University, Park, PA  
J. Rand McNally, Jr., Oak Ridge National Laboratory, Oak Ridge, TN  
R. Moir, Lawrence Livermore National Laboratory, Livermore, CA  
D. B. Montgomery, Massachusetts Institute of Technology, Cambridge, MA  
O. B. Morgan, Oak Ridge National Laboratory, Oak Ridge, TN  
K. Moses, TRW, Redondo Beach, CA  
T. Ohkawa, GA Technologies, San Diego, CA  
D. J. Paul, Electric Power Research Institute, Palo Alto, CA

M. Peng, Oak Ridge National Laboratory, Oak Ridge, TN  
M. Porkolab, Massachusetts Institute of Technology, Cambridge, MA  
R. Post, Lawrence Livermore National Laboratory, Livermore, CA  
F. Powell, Brookhaven National Laboratory, Upton, Long Island, NY  
M. Prelas, University of Missouri, Columbia, MO  
J. Rawls, GA Technologies, San Diego, CA  
F. Ribe, University of Washington, Seattle, WA  
A. Robson, Naval Research Laboratory, Washington, D. C.  
P. Rose, Mathematical Sciences Northwest, Bellevue, WA  
R. Rose, Westinghouse Electric Corporation, Pittsburgh, PA  
M. N. Rosenblueth, Institute for Advanced Study, Princeton, NJ  
J. R. Roth, University of Tennessee, Knoxville, TN  
P. H. Rutherford, Princeton Plasma Physics Laboratory, Princeton, NJ  
T. Samec, TRW, Redondo Beach, CA  
J. Schmidt, Princeton Plasma Physics Laboratory, Princeton, NJ  
K. H. Schmitter, Max Planck Institute fur Plasmaphysik, Garching, West Germany  
F. R. Scott, Electric Power Research Institute, Palo Alto, CA  
J. L. Scott, Oak Ridge National Laboratory, Oak Ridge, TN  
E. C. Selcow, Columbia University, New York, NY  
A. Sessler, University of California, Berkeley, CA  
G. Shuy, University of California, Los Angeles, CA  
W. M. Stacey, Jr., Georgia Institute of Technology, Atlanta, GA  
W. Stodiek, Princeton Plasma Physics Laboratory, Princeton, NJ  
S. Tamor, Science Applications, Inc., La Jolla, CA  
F. H. Tenney, Princeton Plasma Physics Laboratory, Princeton, NJ  
M. Youssef, University of California-Los Angeles  
L. M. Waganer, McDonnell Douglas Astronautics Company, St. Louis, MO  
Library, Centre de Etudes Nucleaires de Fontenay, France  
Library, Centre de Etudes Nucleaires de Grenoble, France  
Library, Centre de Etudes Nucleaires de Saclay, France  
Library, Centre de Recherches en Physique des Plasma, Lausanne, Switzerland  
Library, FOM-Institute voor Plasma-Fysika, Jutphass, Netherlands  
Library, Joint Research Centre, Ispra, Italy  
Library, Japan Atomic Energy Research Institute, Ibaraki, Japan  
Library, Max Planck Institute fur Plasmaphysik, Garching, Germany  
Library, Culham Laboratory, UKAEA, Abingdon, England  
Library, Laboratorio Gas Ionizati, Frascati, Italy